Understanding Coastal and Nearshore Changes in the Area of Thorpeness (Suffolk, UK)

A summary of key findings of the PhD research 'Understanding the Dynamics of a Mixed Sand and Gravel Coastline: A Multi-Method Approach'

Produced by

Dr John Atkinson, PhD Researcher, atkinsonj@bournemouth.ac.uk

Dr Luciana S. Esteves, Associate Professor, lesteves@bournemouth.ac.uk

Bournemouth University

Faculty of Science and Technology

Bournemouth University

Talbot Campus, Poole, Dorset, BH12 5BB, UK

Phone: +44 (0) 1202 9 62446

November 2019

VERSION HISTORY

Version	Changes
V1	Original
V2	Changes in beach management descriptions (Section 3.2 and Figure 6)
V3	Amended volume calculations in Section 4.

EXECUTIVE SUMMARY

This report summarises the key findings of the research undertaken by Bournemouth University in collaboration with the National Oceanographic Centre Liverpool, as part of a PhD studentship co-funded by the university, Suffolk Coastal District Council and Mott MacDonald. The research benefitted from and extended the data collected and analysed under the project *X-band radar and evidence-based coastal management decisions* (X-Com) funded by the Natural Environment Research Council (reference NE/M021564/1). The main aim of this research was to advance the understanding of coastal and nearshore changes in the area of Thorpeness (Suffolk, East Anglia) to inform coastal management decisions.

The area is a mixed sand and gravel system with a complex underwater and coastal geology. The research involved the application of a range of methods to quantify magnitudes and trends of coastal and nearshore changes and to identify the factors influencing these changes, particularly the ones leading to coastal erosion. These methods included: remote sensing through X-band radar to quantify nearshore changes; traditional and novel fieldwork techniques to measure beach changes and sediment characteristics; and numerical modelling to calculate longshore sediment transport (LST) rates and to assess the effects of different wave and nearshore conditions.

The analysis of offshore wave data obtained between Jun-2006 and Mar-2018 indicates a bimodal wave direction, as waves approach dominantly from two directions: 43% of the wave records were from a northerly direction (mainly NNE) and 43% from a southerly direction (mostly SSW). In most years, southerly waves were more frequent than northerly waves; differences in the percentage of waves approaching from a northerly or southerly direction each year varied between 2% and 25%. Southerly waves were also dominant in most winters. However, the proportion of waves from the two dominant directions varies greatly at a range of time-scales. For example, in some winters southerly waves represented 79% of all records (2013-2014) and in others only 32% (2008-2009).

The data obtained from fieldwork (Aug-2016 to Mar-2018) and the analysis of beach profile data from the Environment Agency monitoring programme (since Jan-2009) highlighted the great variability in beach characteristics and response within distances as short 300 m alongshore. Analyses of beach changes between January 2009 and March 2018, along five cross-shore transects representing the range of morphologies in the study area, evidenced that beach growth (+9% of initial cross-sectional area) occurred only at Transect A (at the ness, north of the study area). During the same period, all other transects had eroded, losing from 20% (Transect E, south of the study area) to 60% (Transect C, unprotected sandy cliffs) of their initial cross-sectional area.

The results raised two main areas of concern. In March 2018, Transect D (across coastal protection works at Thorpeness) showed a condition of sediment depletion almost as critical as the one observed in 2010 after a storm had exposed the gabions built in the 1970s. Here, the placement of gabions and geobags has offered some protection to the properties on the clifftop but have also narrowed the beach and cut sediment exchange from the upper beach, enhancing exposure and susceptibility to erosion. The geobags seemed to have created a ‘terminal groyne’ effect, which may be linked to an increase in erosion in the area to the north of the village (around Transect C), where the cliff retreated 12 m between Aug-2016 and Mar-2018. The erosion trend observed south of the ness (Transect B) is also of concern. A 60% reduction in the profile area was

observed between 2014 and 2017. This area had been used in the past as a source of gravel extracted to recharge the beach at Thorpeness. Despite some recovery observed since 2017, extraction of material from this area should be avoided until monitoring demonstrates accretion continues. It would be beneficial to investigate the minimum profile area that needs to be maintained to ensure any artificial removal of material will not be detrimental.

Numerical modelling simulations indicate that, over the longer-term and during periods dominated by southerly waves, the ness benefits from a sediment convergence, contributing to its stability and growth. Sediment eroded from Thorpeness is likely to be transported northwards and deposited around the ness below the MHWS. The mean annual longshore sediment flux northward is estimated in the order of 32,000 $m^3\ a^{-1}$ of sand and 3,500 $m^3\ a^{-1}$ of gravel. Therefore, the ness may provide a relatively more stable source for small-scale extraction of sediment, particularly if restricted to areas below MHWS. However, periods dominated by northerly waves (such as from Dec-2009 to Feb-2010), a sediment divergence can occur just north of Thorpeness, enhancing localised erosion around the area of Transect C. Under these conditions, sediment along Thorpeness will be transported southward instead of northward. The timing and scale of any gravel extraction must be carefully planned to ensure that the amount of material removed from the ness can be replaced naturally at time-scales that can offer the coastal protection required at Thorpeness without having a detrimental impact elsewhere.

In the study area, there is a considerable variability alongshore in the way beaches respond to the same offshore wave conditions. This variability is driven by alongshore differences in wave energy and/or rates of longshore sediment transport, caused by how waves change when they interact with the seabed in the nearshore. In the study area, the nearshore shows a complex bathymetry due to the presence of Coralline Crag ridges, large mobile bedform features (such as sand waves) and a dynamic oblique bar off the ness. Localised changes in nearshore bathymetry can lead to concentration of wave energy and/or changes in the angle in which they approach particular stretch of the coast. When waves approach the coast at a higher angle and with more energy, sediment transport increases and erosion is enhanced. It is important then to identify where nearshore changes are largest, the magnitudes and time-scale of these changes and whether they may lead to localised coastal erosion.

To assess changes in bathymetry it is necessary to have measurements of the water depth across the area of interest at different dates. Most often, the measurements are obtained by undertaking bathymetric surveys using a multibeam echo sounder attached to a boat. The high costs of obtaining multibeam bathymetry restrict the frequency and coverage of data. Remote sensing techniques offer an alternative to obtain data more frequently and over larger areas at lower costs. Marine X-band radars can capture the backscatter from changes in the sea surface. These data can be used to measure waves and, through calculations based on wave theory, estimate the water depth. As any other remote sensing technique, *in situ* measurements are needed to calibrate the measurements and assess their accuracy.

Between Aug-2015 and Apr-2017, an X-band radar was installed at Thorpeness to assess changes in the nearshore bathymetry. A multibeam survey undertaken concomitantly with radar data in Jan/Feb-2017 allowed determining that the radar-derived bathymetry is accurate within ±0.5 m when data quality conditions are met. Therefore, the assessment is only warranted in areas where changes in bathymetry are larger than this error band. Additionally, wave conditions must be favourable for capturing good quality radar data. Favourable conditions include wave heights above 1 m, approaching the radar view at a low angle and winds exceeding 3m/s (to create the sea surface roughness). Following careful analysis, 53 'blocks' of data were found to meet the quality control criteria to produce bathymetric maps. However, between most of them changes were within the error of the method, limiting the analysis to a few periods.

X-band radar data enabled analysis of bathymetric changes at time-scales varying from 23 days to six months (or longer). Net volume changes can be considerable (29,735 m^3) even in periods of few weeks, as observed between 21-Jan-2017 and 13-Feb-2017. The largest changes were observed in two nearshore areas adjacent to each other and showing opposite changes. Area 1 is located off the ness, where an oblique bar extending 500 m in a southeast direction can form and then erode resulting in bathymetric changes of up to 2 m. Area 2, just south of Area 1, extends 400 m alongshore off Transects B and C. The position of the ness and the areas of large nearshore changes seem to be controlled by the underlying geology, particularly the Coralline Crag ridges.

The largest nearshore changes occurred between 11-Oct-2015 and 6-Feb-2016, when an overall net accumulation of 74,000 m^3 of sediment is estimated across the study area. Deposition (112,000 m^3) was observed within Area 1 and erosion in Area 2 (-26,000 m^3) and along the shore between Transects C and E (Area 3, -12,000 m^3). Southerly waves dominated during this period, including the highest waves. These waves lead to nearshore erosion in the south and longshore transport moving sediment northwards to Area 1, where sediment convergence results in the build-up of the oblique bar and beach accretion at the ness. Through the analysis of two multibeam surveys, changes of similar magnitudes were observed between Jul-2014 and Jan-2017. Although radar-derived bathymetry is not as accurate as multibeam surveys, radar data enabled assessment of nearshore changes at frequencies that would be prohibitively expensive by other means. For example, the analysis showed that magnitudes of changes observed over 2.5 years between multibeam surveys, can actually occur at much shorter intervals (4 months).

Changes in the nearshore bathymetry can affect the direction and volume of longshore transport at a range of temporal scales. For example, south of Sizewell, the mean annual LST flux reverses to a northward direction along a short stretch when nearshore conditions are as in Jan-2017 (the oblique bar is less developed, and Area 2 is shallower/accreted). Within the time-frame of a winter season, the nearshore conditions have some impact on the magnitude of LST, which can differ up to 5,000 m^3 when northerly waves dominate and less than 2,500 m^3 when southerly waves dominate. In winters dominated by southerly waves, the position of the sediment convergence at the ness is slightly to the north when the nearshore conditions are similar to Jul-2014 (the oblique bar is more developed and Area 2 is deeper).

CONTENTS

Executive Summary i
Contents iv
Abbreviations and Nomenclature v
Acknowledgement of Funding Sources v
1. Introduction 1
2. Wave Climate 3
3. Magnitudes and Trends of Coastal Change 5
  3.1. Changes in Beach Volume 6
  3.2. Beach Changes Trends (Jan 2009-Mar 2018) 8
  3.3. Beach Changes at the Ness 11
  3.4. Beach Changes North of Thorpeness (Retreating Cliff Face) 13
  3.5. Beach Changes at Thorpeness 13
4. Changes in the Nearshore 15
5. Effects of the Bimodal Wave Direction 18
6. Sediment Transport 20
7. Will an Increase In the Proportion of Sand Result In Enhanced Erosion? 24
  7.1. A Cost-Effective Sampling Strategy 26
  7.2. Complexity of Results 27
8. Summary of Key Findings 29
References 31
Appendix A: Digital Terrain Models and Changes In Beach Volume 32
Appendix B: Access to Data 35
Appendix C: Calibration of the Radar-Derived Bathymetry 36

ABBREVIATIONS AND NOMENCLATURE

CAM	**Coastal Area Model**
DGPS	Differential Global Positioning System
Dir_P	Peak Wave Direction
DTM	Digital Terrain Model
EA	Environment Agency
g	Acceleration due to gravity
H_s	Significant Wave Height
H_{sb}	Significant wave height at wave breaking point
LST	Longshore Sediment Transport
MHWS	Mean High Water Springs
MLWS	Mean Low Water Springs
MWL	Mean Water Level
MSG	Mixed Sand and Gravel
MSGB	Mixed Sand and Gravel Beach
n	Number of samples within statistical test
ODN	Ordnance Datum Newlyn
p	Significance of statistical test
Q	Volumetric Longshore Sediment Transport rate (m^3 s^{-1})
r	Pearson correlation coefficient
SCDC	Suffolk Coastal District Council
$\tan\beta$	Beach slope
X-com	X-band radar and evidence-based coastal management
θ	Wave angle relative to beach
ρ_s	Sediment Density

ACKNOWLEDGEMENT OF FUNDING SOURCES

The authors would like to thank Bournemouth University, Suffolk Coastal District Council and Mott MacDonald for co-funding the fieldwork and the PhD studentship of John Atkinson, which made this research possible. In particular, we would like to show appreciation for the support and assistance provided by Bill Parker and Paul Patterson from the Coastal Partnership East, and the co-supervision offered by Professor Jon Williams (from Mott MacDonald) and Dr Paul Bell (from the National Oceanography Centre Liverpool). For the help received during fieldwork, we thank the staff from the Coastal Partnership East (Paul Patterson, Nick Reeves, Becky Koelher, Lucy Williams), and colleagues Dr Leo Clarke, Lucy Goodman, Alex Wilcocks and James Bell. The radar data analysed in this research were collected during the *X-band radar and evidence-based coastal management decisions* (X-Com) project funded by the Natural Environment Research Council (reference NE/M021564/1). Throughout this research, particularly during the X-Com project, we were grateful for the support received from local residents and property owners, particularly Fred Monson, Lucy Ansbro, Glen Ogilvie, Mike Chandler and Sheila Moore.

1. INTRODUCTION

Quantifying magnitudes of coastal change and understanding drivers of temporal and spatial variability are paramount to support sound coastal management decisions. Worldwide, coastal management decisions are often impaired due to the poor quality and availability of information about the local processes. Thorpeness is a coastal village in Suffolk (Figure 1), where cliff and beach erosion threaten beachfront properties, despite long-term erosion rates being considerably lower than other areas in East Anglia. More recently, concerns were raised after coastal protection structures were exposed during storms in 2010 and 2013. Studies commissioned by the Suffolk Coastal District Council (Mott MacDonald 2014, 2016) suggested that: (a) storm conditions may be causing concentration of wave energy along a short stretch of the North End Avenue beach frontage; (b) it would be unwise to invest in further coastal protection structures until the factors causing this localised erosion are better understood; and (c) beach recharge would be a more effective and sustainable option if suitable sources of sediment (gravel) are identified.

To address the knowledge gaps impairing informed coastal management decisions, a partnership was formed between Suffolk Coastal District Council, Mott MacDonald, Bournemouth University and the National Oceanographic Centre with valuable support from local residents. This partnership enabled the development of two interlinked research projects aiming to advance the understanding of drivers and rates of coastal change in the area of Thorpeness and how they vary along the coast and through time. As part of the innovative project *X-band radar and evidence-based coastal management decisions* (hereafter X-Com) funds were secured from the Natural Environment Research Council (reference NE/M021564/1) to install a land-based marine X-band radar in Thorpeness (Figure 1c) from August 2015 to April 2017. A PhD research (Atkinson 2019), conducted from January 2016 to April 2019, analysed in detail the data obtained during the X-Com project in combination with beach surveys to understand the linkages between changes in nearshore bathymetry, beach response and meteorological and oceanographic (hereafter metocean) conditions. Obtaining data from the nearshore is generally complex and costly; this research used a combination of methods to overcome these difficulties.

X-band radar data provides a range of information about waves, currents and bathymetry across a relatively large area (2-3 km radius), day and night (typically every 30 minutes) and at all weather conditions (except very heavy rain). Therefore, the X-band radar provides frequent and regular data over a much larger area and at a fraction of the cost of traditional in *situ* measurements. However, there are limitations inherent to the method, and these need to be understood and quantified to ensure the data suit the intended applications. The analysis of X-band radar data involved time-consuming processing and complex quality control, but results were valuable to understand where and when changes in nearshore bathymetry occur and how they relate to beach erosion.

The quantification of beach changes and how they vary along the coast and through time was based on data obtained during 15 visits to the study area between January 2016 and March 2018. These data consisted of topographic surveys using a combination of technologies and sediment samples, which required time-consuming laboratory analysis and laborious data processing. Additionally, beach profile data collected by the Environment Agency (EA) since 2009 were analysed to identify longer-term trends of shoreline changes. Results show that, in this study site, beach changes vary greatly even within short distances (<300 m) alongshore both at short (before and after storms) and longer (within a decade) temporal scales. Field and radar data were then used to inform numerical modelling simulations testing how wave energy and sediment transport vary as a result of different wave conditions and how these are affected by changes in nearshore bathymetry.

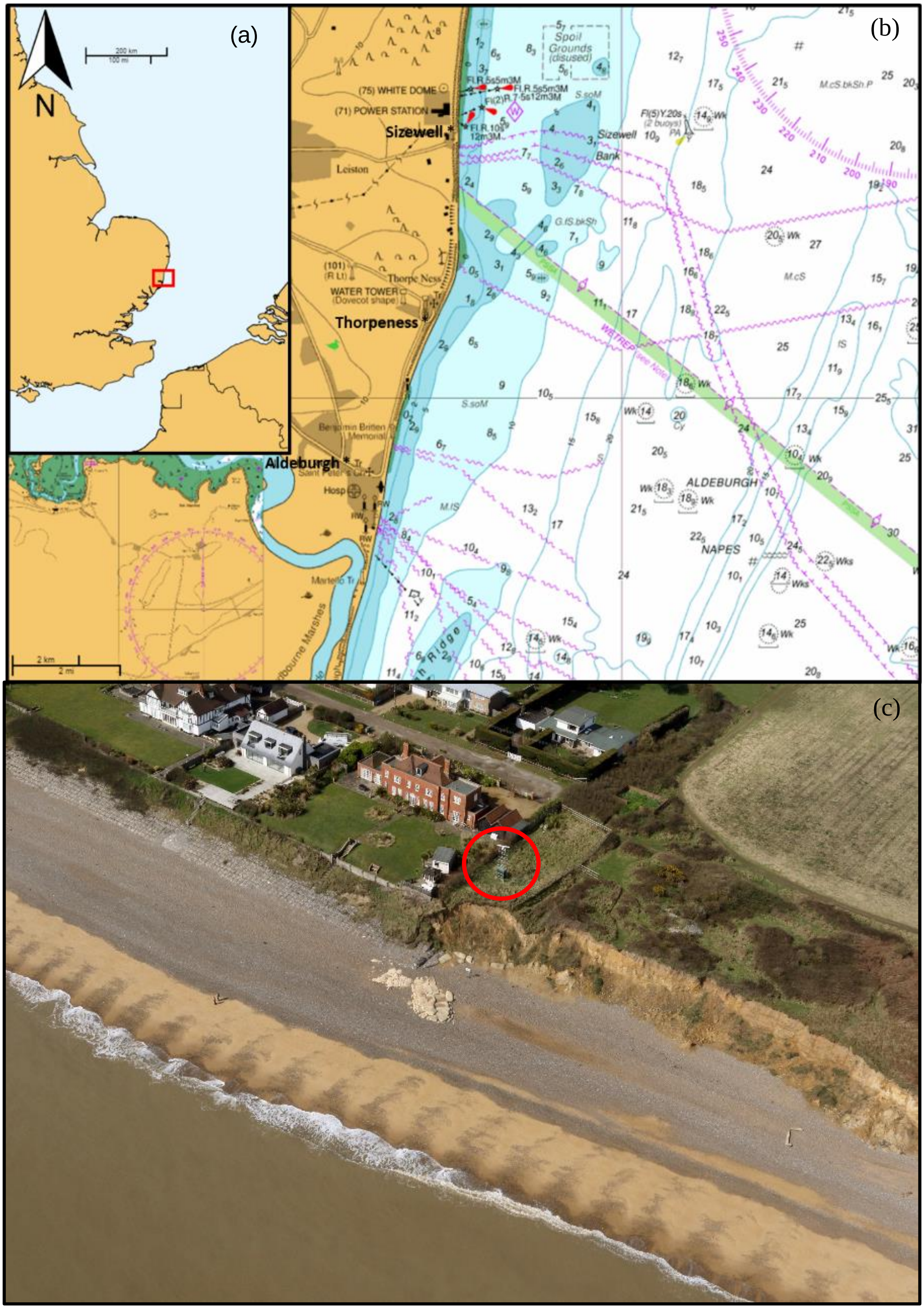

Figure 1. (a) Location of the study area at the coast of East Anglia (eastern UK) and (b) Thorpeness village (coast of Suffolk) between Aldeburgh and Sizewell nuclear power plant showing nearshore bathymetry (Digimap 2004). (c) Aerial photography showing the radar position on top of the cliff at the northern end of Thorpeness village (13-Apr-2016, Photo by Mike Page).

This report presents the key findings of the research described above. Section 2 summarises the wave climate measured offshore the study area by the West Gabbard wave buoy. The section highlights that periods in which southerly (SSW) or northerly (NNE) waves dominate do not follow seasonal or interannual patterns. Section 3 describes magnitudes and trends of coastal change and how they vary within the study area and through time. The analysis focused on three contrasting areas: the Thorpeness beach frontage, the eroding soft cliffs north of Thorpeness and the gravel foreland (known as the ness) between Thorpeness and Sizewell. Section 4 quantifies changes in the nearshore at a range of temporal scales through the analysis of bathymetry multibeam surveys and radar data. Section 5 analyses the interactions between beach, nearshore changes and wave conditions. Section 6 investigates these interactions through numerical modelling to better understand how different waves and nearshore conditions affect the rates and direction of longshore sediment transport. Section 7 analyses sediment data to identify whether changes in the proportion of sand and gravel has an effect on beach mobility. Section 8 provides a brief overview of the key findings.

2. WAVE CLIMATE

Quantifying the mean and extreme values of metocean conditions at the study area across a range of time-frames is essential to understand: (a) how the coast may change under different conditions and (b) how often different conditions are likely to cause significant coastal changes. While significant coastal changes are often associated with storm impacts, considerable changes can also result from prolonged moderate conditions. Characterising the wave climate during the duration of the project can help understand how observed conditions compare to previous years. The analysis presented here is based on offshore data recorded by the West Gabbard buoy, located about 40 km southeast of the study area.

From Jun-2006 to Mar-2018, a strong bimodality in the direction of offshore waves was evident. Waves approached from two dominant directions (Figure 2a): 43% of the records were from a northerly direction (300–60°), mainly NNE, and 43% from a southerly direction (120–240°), mostly from the S-SW (Table 1). In most years (8 out of 11), southerly waves were more frequent than northerly waves (Table 1). Differences in the percentage of waves approaching from a northerly or southerly direction vary between 2-3% (e.g. 2010, 2013, 2015, 2017) and 25% (more northerly waves in 2011). Differences are larger when the analysis focuses on winter months only, varying from about 4% more northerly waves in 2012-2013 to as much as 66% in 2013-2014, when 79% of the time waves approached from a southerly direction and 13% from a northerly direction (Table 1).

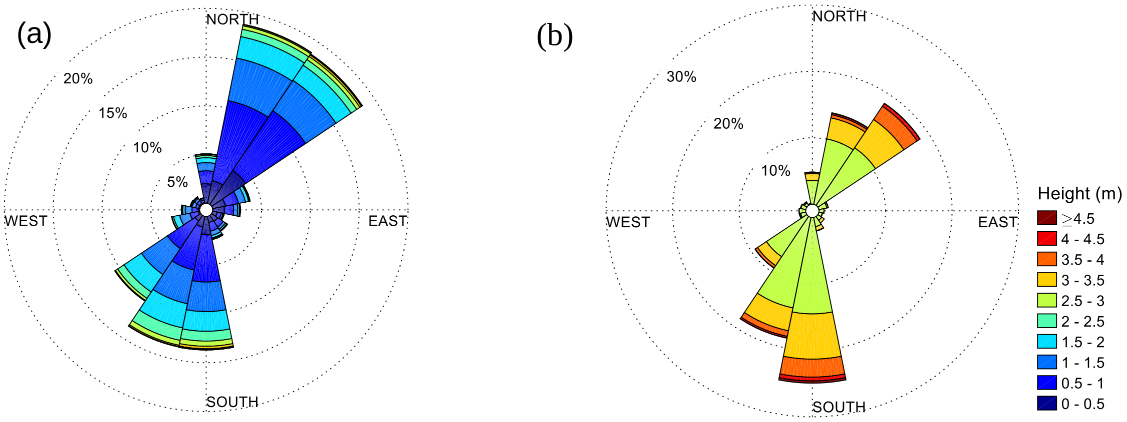

Figure 2. West Gabbard buoy wave roses for (a) all waves and (b) waves of H_s > 2.5 m, showing the percentage of waves of different heights (H_s) that approach from different directions in the period Jun-2006 to Mar-2018 (168685 records, 98% data coverage).

Table 1. Annual and winter (DJF) statistics for the 95th percentile, maximum and mean significant wave height (Hs) and the proportion of records from the West Gabbard 1 and 2 buoys approaching from a northerly (300–60°) or southerly (120–240°) for all waves and waves of H_s > 2.5 m.

	Significant Wave Height H_s (m)			**All waves (from direction)**		**H_s >2.5 (% of all waves)**	**H_s> 2.5m (from direction)**	
Year	95th	max	mean	N (%)	S (%)		N (%)	S (%)
All Data	2.32	5.25	1.09	43.44	43.02	3.56	1.45	1.87
2007	2.23	4.09	1.13	32.44	48.77	3.35	0.50	2.82
2008	2.41	5.25	1.14	49.28	37.93	3.07	1.66	1.22
2009	2.23	5.06	0.96	39.17	45.98	4.66	1.49	2.88
2010	2.32	4.55	1.07	41.60	43.88	2.86	1.25	1.55
2011	2.14	4.09	1.05	57.09	31.87	4.16	3.16	0.86
2012	2.23	4.24	1.04	36.46	49.48	1.59	0.26	1.20
2013	2.51	5.06	1.12	42.62	45.99	3.28	1.31	1.59
2014	2.32	4.39	1.10	48.98	38.03	5.06	2.71	2.07
2015	2.28	4.42	1.11	42.88	45.63	3.82	0.43	3.03
2016	2.37	4.83	1.11	38.18	47.78	3.07	0.42	2.48
2017	2.15	4.50	1.02	42.32	45.04	3.93	1.59	2.17
Winter (DJF)								
2006-07	2.71	4.09	1.39	33.16	52.13	7.72	0.48	6.75
2007-08	2.61	4.72	1.37	23.94	57.73	7.48	0.32	6.56
2008-09	1.89	3.94	0.73	53.42	32.30	2.39	0.46	1.90
2009-10	2.82	5.06	1.36	55.49	32.72	7.11	6.50	0.40
2010-11	2.32	4.55	1.24	49.82	38.79	4.14	3.04	1.11
2011-12	2.51	3.94	1.32	34.96	46.82	6.02	1.98	3.25
2012-13	2.51	3.40	1.33	44.28	40.72	5.13	1.42	3.12
2013-14	3.04	5.06	1.61	12.94	79.34	15.14	0.15	14.64
2014-15	2.57	3.82	1.39	38.61	44.36	6.04	1.23	4.08
2015-16	2.78	4.04	1.57	20.63	70.35	10.21	1.65	8.24
2016-17	2.23	3.48	1.08	32.26	51.54	2.13	1.18	0.58
2017-18	2.67	4.18	1.39	36.78	42.60	7.27	2.75	3.36

Higher waves (significant wave height, Hs, >2.5 m) represented 3.6% of all records. These waves approached dominantly (53% of records) from the S-SW (Figure 2b); 41% approaching from the N-NE. Waves Hs>2.5 m are more frequent during the winter, 2.1-15.1% of winter records contrasting with 1.6-5.1% of all records. The wave height statistics (Table 1) indicate that the mean Hs and the 95th percentile tend to be higher in the winter months; however, the highest waves (max Hs) occur outside the winter (generally in the autumn).

From August 2015 to April 2018 (the period of data collection), interannual variability in the dominant wave direction was relatively low (45-48% of records were southerly waves and 38-46% northerly waves). Dominance of wave direction was more pronounced in the winters of 2013-2014 and 2015-2016; when southerly waves occurred in 79% and 70% of all records, and 15% and 10% of Hs>2.5m records, respectively (Table 1).

3. MAGNITUDES AND TRENDS OF COASTAL CHANGE

Topographic surveys are widely used to assess changes in beach morphology and patterns of erosion and accretion. Topographic data were obtained through laser scanning and DGPS (Digital Global Positioning System) surveys of beach profiles collected from 2016 to 2018, although the analysis also included EA data collected from 2009 (Table 2). The EA beach monitoring programme has been gathering topography data along cross-shore transects in the study area twice a year since 2009, sometimes more often to cover periods of large changes, such as during beach nourishment projects.

Table 2. Dates of topographic surveys analysed in this section (GPS surveys indicated as EA were obtained from the Environment Agency).

Date	Beach Profile Surveys	Laser Scanning
07-Jan-2009	EA	
27-Jul-2009	EA	
07-Jan-2010	EA	
20-Jul-2010	EA	
27-Jan-2011	EA	
22-Jun-2011	EA[a]	
22-Dec-2011	EA	
26-Jul-2012	EA	
06-Feb-2013	EA	
18-Jul-2013	EA	
08-Feb-2014	EA	
05-Aug-2014	EA	
29-Jan-2015	EA	
05-Aug-2015	EA	
02-Feb-2016	EA	
26-Jul-2016	EA	
03-Aug-2016	x	x
22-Oct-2016	x[b]	x
06-Dec-2016	x	x
09-Jan-2017	x[c]	
19-Jan-2017	x	x
13-Feb-2017	x	x
21-Mar-2017	x	x
27-Jun-2017	x	x
20-Jul-2017	x	
27-Sep-2017	x	x
16-Jan-2018	x	x
26-Feb-2018	x	
07-Mar-2018	x	
27-Mar-2018	x	

[a] Transect A and C measured on 8–9 June; [b] unavailable for Transect C; [c] available only for Transects A and B.

Five transects from the EA coastal monitoring scheme were selected for analysis here as they reflect the distinct local settings and morphological features of the study area. These five transects are herein identified sequentially from north to south as Transects A to E (Figure 3):

a. Transect A (EA profile TN007) is located at the north end of the study area crossing the gravel ridges of the ness.
b. Transect B (EA profile TN013) crosses the south flank of the ness, where a gravel berm is often prominent and backed by a vegetated and eroding cliff talus.
c. Transect C (EA profile TN017) is characterised by the presence of a rapidly retreating soft cliff, a gravel upper beach, and a sandy lower beach (although temporal variations occur).
d. Transect D (EA profile TN021) crosses a local erosion “hot spot”, where the beach profile is influenced by gabions, geobags, and gravel nourishment. The gabions were placed in the 1970s and the geobags in 2011, after a storm exposed and damaged the gabions in the spring of 2010. These structures are periodically exposed during storms, with gravel nourishment occasionally used to restore the beach profile and cover the structures.
e. Transect E (EA profile TN026) is located south of the coastal protection structures, approximately at the centre of the village’s seafront housing.

Figure 3. (a to e) Beach morphology along transects A to E, respectively (Photos by L.S. Esteves) and (f) their approximate location within the study area shown on an oblique aerial photograph taken after an intense erosion event in 2010 (Aerial photography by www.mike-page.co.uk).

3.1. Changes in Beach Volume

Laser scan surveys of the beach and cliff face along the village frontage were used to produce digital terrain models (DTMs) to facilitate the visualisation of how beach levels change both cross-shore and alongshore. Assessing differences in beach levels between two DTMs of the same area measured at different times can provide information about the areas of largest changes (beach lowering or accretion) and how much sediment (sand and gravel) has moved. Changes in sediment volume above mean high water springs (MHWS) in the scanned areas between 03-Aug-2016 and 24-Jan-2018 reached -2624 m^3 (Table 3), suggesting a net loss of sediment. However, there are considerable differences between the changes observed in the northern and the southern sectors, where volume loss (erosion) and gain (accretion) tends to occur, respectively (Figure 4).

Magnitudes of changes vary through time and with the time-scale of the analysis (Table 3). For example, changes at an annual scale varied considerably between the periods 03-Aug-2016 to 27-Sep-2017 and 18-Jan-2017 to 24-Jan-2018. Although in both periods there was net erosion in the north and accretion in the south, magnitudes of changes were considerably different (Figures 4 and 5). Considerable net erosion (-8443 m^3) was observed in the period 03-Aug-2016 to 27-Sep-2017 (Figure 4). and a slight accretion (+398 m^3) in the period 18-Jan-2017 to 24-Jan-2018 (Figure 5). Net changes over a period of around 40 days (06-Dec-

16 to 18-Jan-17) can be of similar magnitude to changes observed over four months (03-Aug-16 to 06-Dec-16) reaching erosion of more than 3000 m^3 in the northern sector and around 4000 m^3 across the area (Table 3).

Table 3. Changes in sediment volume above MHWS (net and daily averages) in the northern and southern sections and overall across the beach and cliff face area surveyed by laser scanner at a range of time scales.

Period		**Net change (m^3)**			**Mean net change per day ($m^3 day^{-1}$)**		
		North	South	Overall	North	South	Overall
03-Aug-16	24-Jan-18	-5672	+3048	-2624	-11	+6	-5
03-Aug-16	27-Sep-17	-9037	+594	-8443	-22	+1	-20
18-Jan-17	24-Jan-18	-2672	+3070	398	-7	+8	+1
03-Aug-16	06-Dec-16	-3414	-924	4338	-27	-7	35
06-Dec-16	18-Jan-17	-3170	-769	-3939	-74	-18	-92
21-Mar-17	27-Jun-17	-924	+650	-274	-9	+7	-3
27-Jun-17	27-Sep-17	+634	+223	857	+7	+2	+9
27-Sep-17	24-Jan-18	-1695	1204	-491	-14	+10	-4

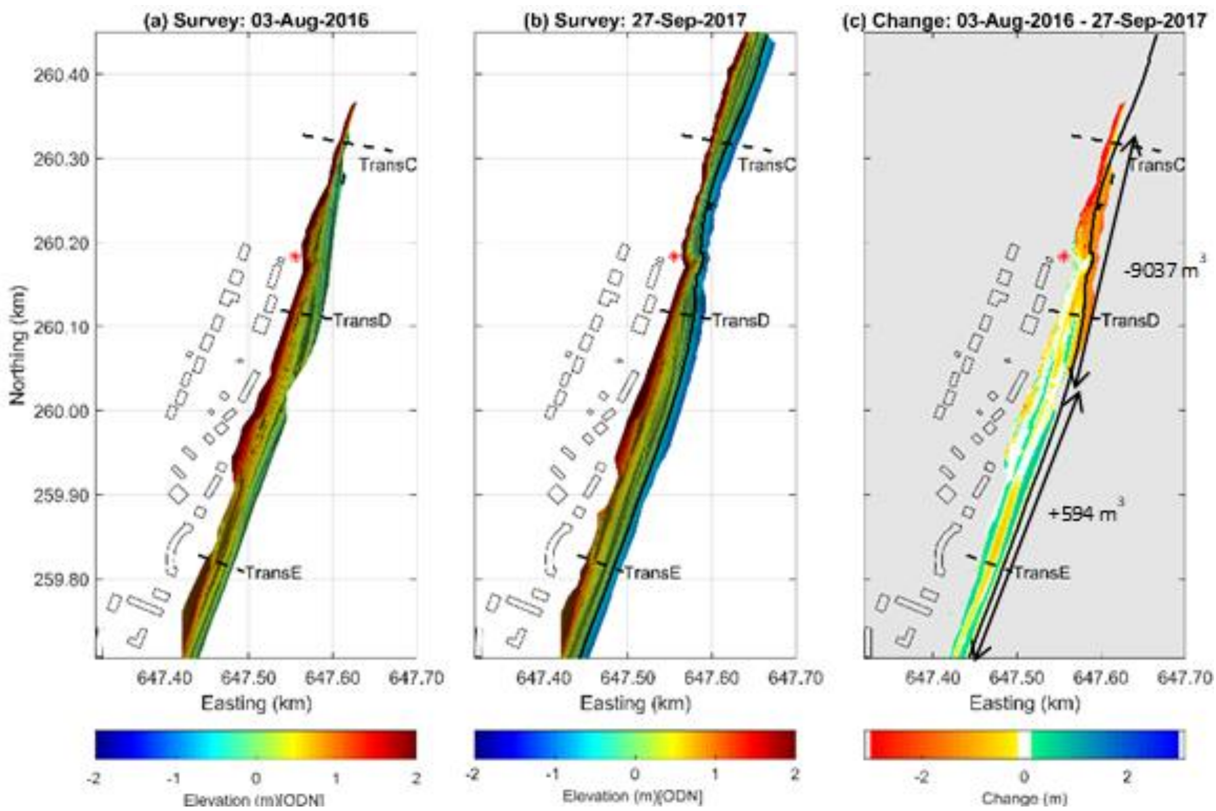

Figure 4. Digital Terrain Models produced from laser scanner data obtained on (a) 03-Aug-2016 and (b) 27-Sep-2017, and (c) changes in elevation between surveys. The values indicate the volume change above MHWS (shown as a black line) at the northern and southern sectors (defined by the arrows alongshore). The position of Transects C, D and E are indicated by dashed lines and the radar by the red star. Contours of buildings are shown to provide points of reference.

In the southern sector, volume changes are related to the movement or formation/deformation of gravel ridges, as evident by the alternating bands of erosion and accretion in the annual changes shown in Figure 4c. The largest volume losses (>-1000 m^3) in the northern sector reflect erosion of the cliff face north of the radar; sometimes enhanced by lowering of adjacent beach levels (Figure 4c), while at other times it may be a source for accretion of beach levels above MHWS (Figure 5c). Erosion around the exposed geobags is evident in annual (Figure 4c) and shorter-term changes (e.g. 21-Mar-2017 to 27-Jun-2017, Appendix A – Digital Terrain Models). At the northern flank they are taking the shape of a 'terminal groyne', seen as a small bulge in the MHWS line in front of the radar position in Figures 4 and 5.

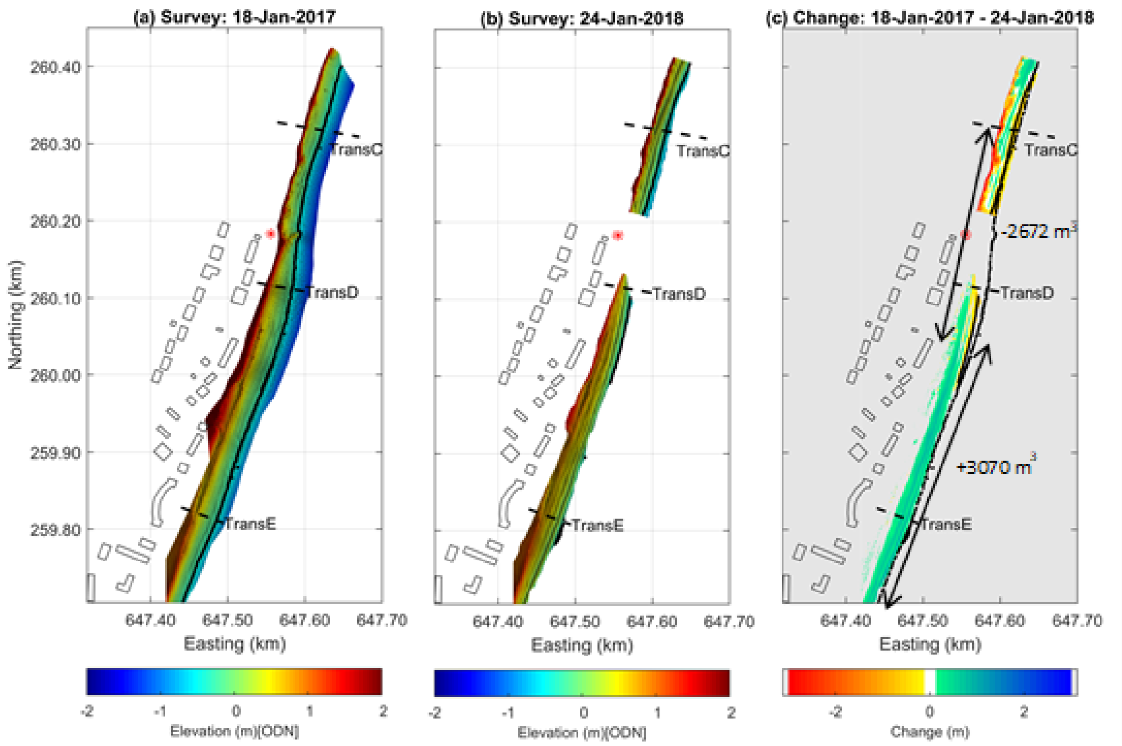

Figure 5. Digital Terrain Models produced from laser scanner data obtained on (a) 18-Jan-2017 and (b) 24-Jan-2018, and (c) changes in elevation between surveys, the values indicate the volume change above MHWS (black line) at the northern and southern sectors (defined by the arrows alongshore). The position of Transects C, D and E are indicated by dashed lines and the radar by the red star. Contours of buildings are shown to provide points of reference.

3.2. Beach Changes Trends (Jan 2009-Mar 2018)

Analyses of changes along the five selected beach transects were conducted based on the changes in beach width and the profile cross-section area. The cross-section area is used as a proxy for changes in volume by assuming that the topography shown is representative for a certain stretch of the coast. Using a simple example: if the beach topography can be assumed to represent the conditions across 5 m each side of a measured transect, the beach volume can be calculated by multiplying the profile area by 10 m. Therefore, in Figure 6, the initial area of Transect A in January 2009 was 208.22 m^2, or an estimated volume of 2082.2 m^3 in 10 m of coastline.

To assess if changes occur in the intertidal area or higher up the beach, the beach width was estimated at mean low water springs (MLWS), mean water level (MWL) and mean high water springs (MHWS). These tidal levels were defined relative to Ordnance Datum Newlyn (ODN):

MHWS = 1.22 m, MWL = 0.16 m, and MLWS = −1.01 m (Mott MacDonald 2014). Similarly, the profile cross-section area was estimated above and between these levels. For consistency, beach widths and profile areas were calculated using a fixed landward boundary in each transect that encapsulated the changes observed across the period of analysis. All data related to the different indicators of beach change calculated in this study can be found in Appendix B. A comprehensive analysis of these data is presented in Atkinson and Esteves (2018).

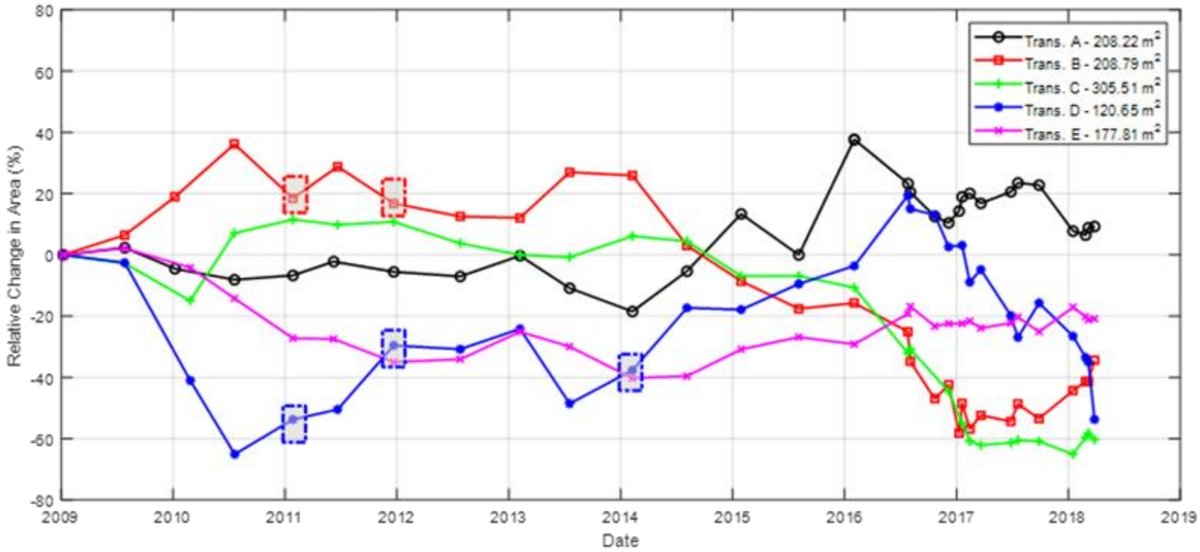

Figure 6. Change in profile area above MLWS for Transects A–E calculated as a proportion of the respective initial area on 07-Jan-2009 shown in the legend. Grey boxes indicate beach nourishment and reprofiling in the area of Transect D, with gravel taken from the area of Transect B.

Descriptive statistics of key indicators (Table 4) provide a general overview of differences and similarities across transects. For example, it is evident that the largest reduction in area (erosion) in all transects occurred when conditions are compared between July (summer) and January or February (winter) but the largest beach retreat (landward movement of the shoreline position) shows variation of this pattern in Transects A and C. The largest increase in area and in beach width occurred when comparing conditions between the winter and the summer, except in Transect A. The maximum and minimum values of both beach width and area not always result from the largest beach growth/accretion and retreat/erosion, respectively, suggesting that gradual changes over prolonged periods can have significant effects. Transect D shows the largest variability in both beach width and area (indicating high beach mobility), while Transect A shows less variability in area and Transect E in beach width. Beach mobility is considered high when the range value (the difference between the maximum and the minimum values) is similar or exceeds the mean value.

The analysis of changes in profile area through time indicates that periods of accretion and erosion were observed in all transects, although with varied timings and durations (Figure 6). Only Transect A (at the Ness, north of the study area) showed a slight (~10%) increase in profile area between January 2009 and March 2018. During the same period, all other transects showed a reduction in profile area of 20% (Transect E, south of the study area) to 60% (Transect C, unprotected sandy cliffs).

The storm that exposed the 1970s gabions along the Thorpeness beach frontage in May 2010 enhanced the erosion trend along Transect D and E, triggered accretion along Transect C and had no major effect along Transects A and B. In July 2010, the area in Transect D reached its most eroded condition during the period of analysis (a 65% reduction of the cross-sectional area in relation to January 2009) and Transect B reached its most accreted condition (almost 40% increase in area). In contrast, the extended stormy period from October 2013 to February 2014 (which exposed the geobags installed in 2011) seemed to have triggered accretion in Transects A, D, and E and erosion in Transects B and C. In 2013 there were prolonged periods of waves higher than 2.5 m, dominantly from a southerly direction; in 2010 higher waves were lower, less frequent and dominantly from the northeast. At different times in 2016/early 2017, trends changed again, switching to erosion in Transects A and D and to accretion or stability in Transects B, C and E. In 2016, the area loss in Transect C was mainly due to cliff retreat.

Table 4. Descriptive statistics summarising changes in beach width and area (and respective dates where relevant) based on dataset 1 for Transects A to E.

Transects	A	B	C	D	E
Beach width at MWL (m)					
Mean	91.1	67.8	70.2	32.6	67.3
Range	42.3	48.8	41.8	31.0	18.0
Minimum	76.0	40.8	47.8	19.3	61.3
	8Feb14	13Feb17	20Jul17	21Jul10	22Dec11
Maximum	118.3	89.5	89.5	50.3	79.3
	2Feb16	20Jul10	27Jan11	26Jul16	27Jul09
Largest beach growth	29.8	12.8	26.5	10.0	5.75
	Aug15 - Feb16	Feb13 - Jul13	Feb10 - Jul10	Feb16 - Jul16	Feb16 - Jul16
Largest retreat	-11.0	-14.0	-15.5	-12.0	-5.75
	Feb16-Jul16	Jul16 - Feb17	Feb16 - Jul16	Jul09 - Feb10	Jul10 - Jan11
Area above MLWS (m^2)					
Mean	214.5	207.9	271.1	88.3	134.0
Range	116.9	194.2	221.1	101.9	75.4
Minimum	169.7	90.1	119.7	42.1	106.2
	8Feb14	13Feb17	13Feb17	21Jul10	08Feb14
Maximum	286.7	284.4	340.8	144.1	181.6
	2Feb16	20Jul10	27Jan11	26Jul16	27Jul09
Largest accretion	78.4	36.1	67.4	27.8	17.7
	Aug15 - Feb16	Jan10 - Jul10	Feb10 - Jul10	Feb16 - Jul16	Feb16 - Jul16
Largest erosion	-35.5	-66.3	-87.6	-46.5	-23.2
	Jul17 - Feb18	Jul16 - Feb17	Jul16 - Feb17	Jul09 - Feb10	Jul10 - Jan11

It is worth noting that, when the geobags were exposed as a result of the erosion caused by the 2013-14 storms, the beach profile along Transect D was in a relatively more accreted condition than in the 2010 event. The geobags were placed seaward of the gabions and, therefore, are more exposed to the wave action. Although the geobags provided protection to the cliff and beachfront properties, their placement resulted in a narrower beach and less natural dissipation of wave energy.

Small-scale nourishment works occurred in the area of Transect D after storms in 2010, 2011, and 2013 with materials (around 1000–1500 m^3) sourced from the area around Transect B and, later on, from an area 200-400 m south of Transect E. Although these works might have helped protecting the already damaged coastal defences, they caused only a small and temporary effect, not affecting the overall trend either in Transect B or D. However, an erosion trend at Transect B started in early 2014, culminating with 60% reduction in the profile area by 2017 (Figure 6). Despite some recovery has been observed since 2017, extraction of material from this area to nourish the beach further south should be avoided until the profile area shows further recovery or studies demonstrate that it would not enhance risk locally or to adjacent areas. The survey in March 2018 at Transect D showed a state of erosion almost as critical as the one observed after the 2010 storm. Identifying suitable and sustainable sources for beach nourishment requires better understanding of the longer-term trends and critical thresholds of beach levels to ensure management interventions will not enhance erosion.

A more detailed analysis of beach topography and morphology indicates that gravel ridges present in the lower parts of the profile (below MHWS) have an important coastal protection role. One (sometimes more) gravel ridges form below the MWL and then migrate up the beach as a response to wave forcing (as the beach is exposed seaward of the ridge and sheltered landwards). In this process they change shape, often losing height and becoming wider, sometimes merging with other gravel ridges above MHWS, where they spread out and lose form. This migration reflects a movement of gravel from areas below MWL to areas above MHWS, resulting in erosion and accretion, respectively. Gravel ridges were observed in all transects but there were differences in their size, how fast they form and migrate, and the effects on profile morphology. A summary of beach changes at the ness (Transect A), the unprotected cliff line north of Thorpeness (Transect C) and the village's urban frontage (Transects D and E) is presented next.

3.3. BEACH CHANGES AT THE NESS

In the period of analysis, the beach width (at MWL) at the ness (Transect A) has varied over 40 m (Table 4, Figure 7a), and changes in elevation reached 3.8 m between 90-110 m cross-shore distance (Figure 7b). In general terms, a reduction of about 15 m in the beach width was observed between 2016 and 2018. However, beach profiles were relatively wider over this period than most measurements pre-2016 (Figure 7a). The beach width on 27-Mar-2018 was very similar to the position measured at the start of the EA monitoring in January 2009.

The ness is characterised by the presence of multiple gravel ridges, which can have steep flanks and be over 1 m high. Here beach retreat occurs as the gravel ridge closest to the waterline migrates up the beach, as observed between late July 2016 and January 2017 and also in the following year. The retreat below MHWS halted when the ridge moved above MHWS. The migration continued until all ridges coalesced, resulting in a higher and flatter beach above MHWS, as seen in 19-Jan-2017. An animation showing the changes in topography along the beach transects can be downloaded from here. The existing data suggests the presence of a single gravel ridge from late winter to the spring, with others forming during the summer (as evident from June–September 2017).

Along Transect B (south of the ness), the beach width varied almost 50 m (Table 4); despite an increase between 2016 and 2018, in this period the beach was narrower (retreated) than at measurements pre-2016 (Figure 8a). Here, the formation and migration of gravel ridges is similar (but faster) than observed along the ness.

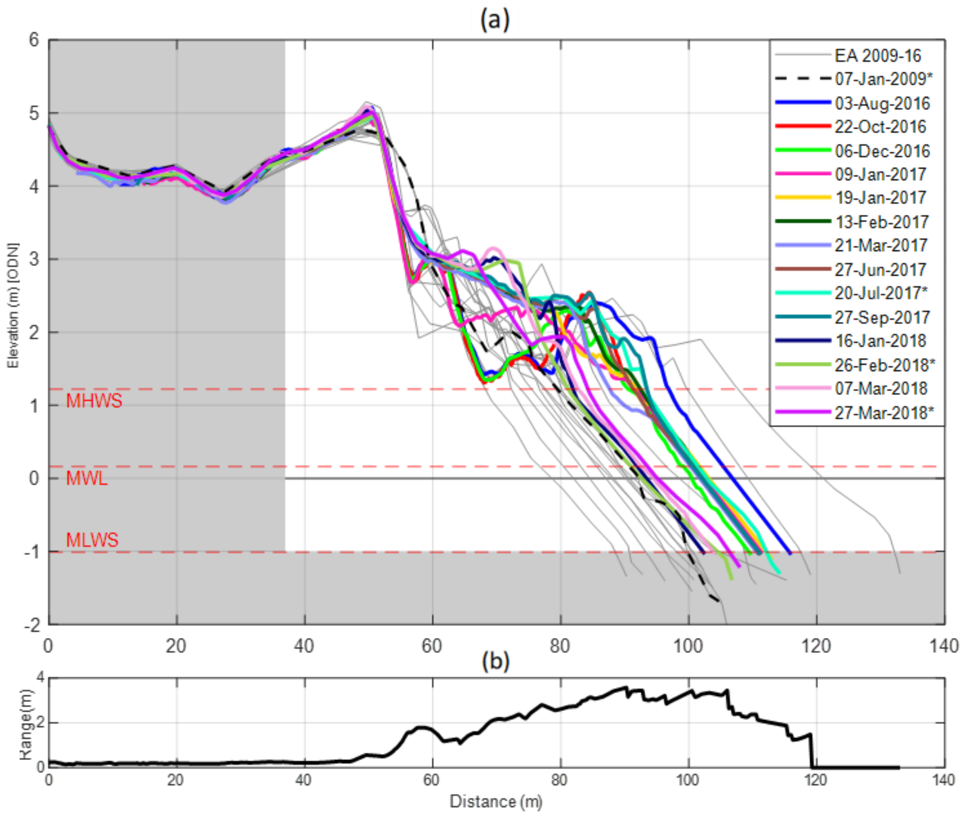

Figure 7. Beach profiles measured along Transect A between January 2009 and March 2018 (a) and maximum changes in elevation along the cross-shore profile (b). For reference, the initial profile (07-Jan-2009) measured by the Environment Agency is shown as a dashed line, while all other EA profiles are shown in grey.

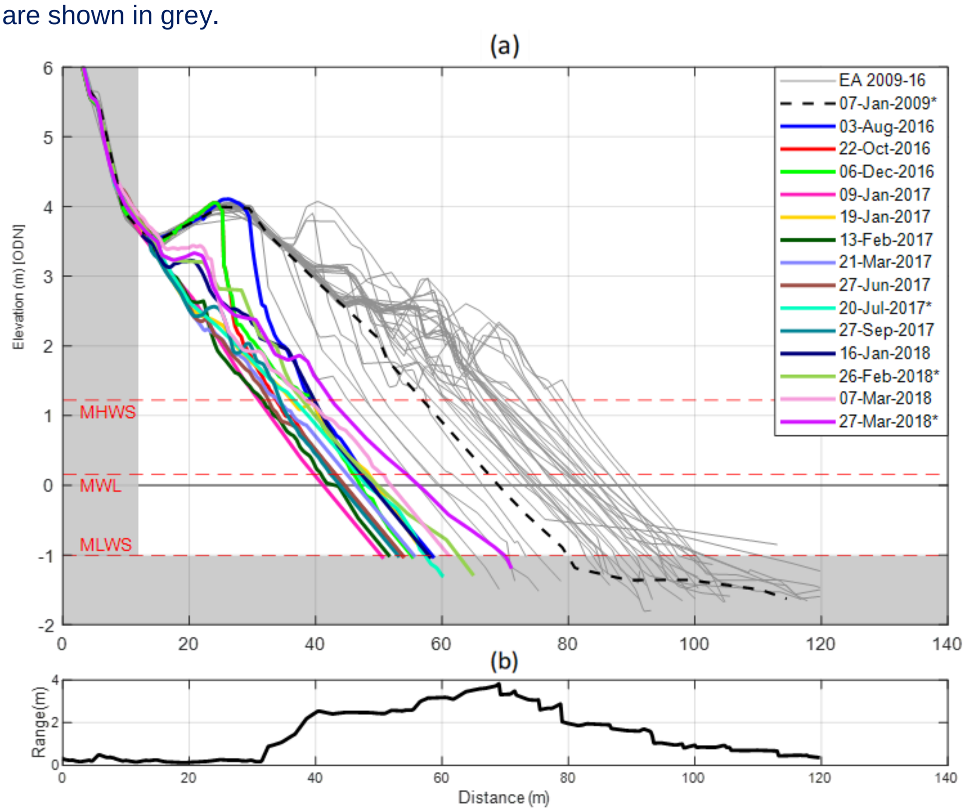

Figure 8. Beach profiles measured along Transect B between January 2009 and March 2018 (a) and maximum changes in elevation along the cross-shore profile (b). For reference, the initial profile (07-Jan-2009) measured by the Environment Agency is shown as a dashed line, while all other EA profiles are shown in grey.

A well-developed gravel ridge present at MHWS in early December 2016 had completely disappeared by 09-Jan-2017, when the profile was greatly eroded (loss of 33 m^2). After erosion, the gravel that was previously found above MHWS became more evenly distributed across the profile. Just 10 days later, a gravel ridge was present below MHWS, with the profile recovering 20 m^2. By 13-Feb-2017, almost all this gain had been lost when the gravel ridge migrated well above the MHWS leaving a flattened and retreated sandy profile below MHWS. A similar pattern of erosion and accretion associated with gravel ridge migration was observed between January and March 2018. Only minor changes were observed between late winter and early summer. Over the summer 2017, the featureless profile remained, with gravel ridges apparent in September.

3.4. Beach Changes North of Thorpeness (Retreating Cliff Face)

North of Thorpeness village, the coast is characterised by a retreating 10-m high cliff face. Between January 2009 and August 2016, the cliff face retreat at Transect C was about 3 m, considerably less than observed since 2016. The cliff face retreated 6 m between 03-Aug-2016 and 06-Dec-2016 (Figure 9a), and a further 5 m by 19-Jan-2017, with tragic consequences. Just a few meters from this transect, cliff failure on 14-Jan-2017 caused the death of a man who was walking his dog along the upper beach when water levels were high. The largest changes in elevation occurred at the cliff face (9 m), while changes in beach levels reached 4 m (Figure 9b).

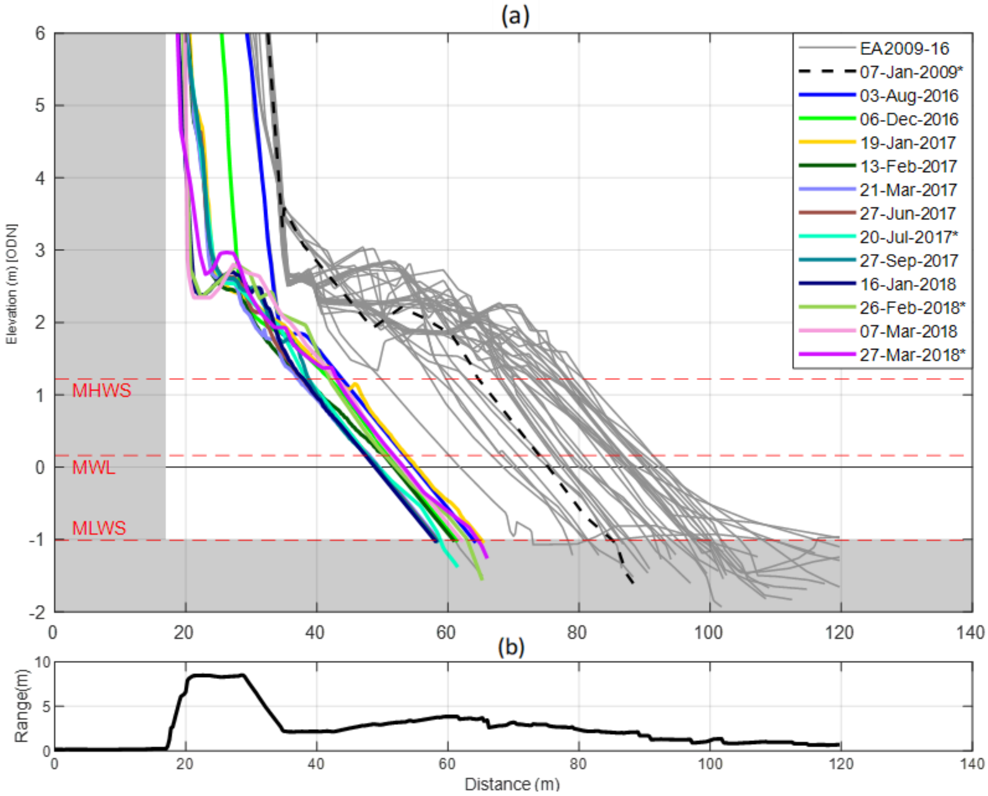

Figure 9. Beach profiles measured along Transect C between January 2009 and March 2018 (a) and maximum changes in elevation along the cross-shore profile (b). For reference, the initial profile (07-Jan-2009) measured by the Environment Agency is shown as a dashed line, while all other EA profiles are shown in grey.

3.5. Beach Changes at Thorpeness

The beach tends to be more stable along the Thorpeness beach frontage than the areas further north. The beach width varied around 30 m at Transect D (Figure 10a) and 20 m at

Transect E (Figure 11a). Generally, beach profiles measured since 2016 tend to be wider than most profiles measured pre-2016. However, on 27-Mar-2018 the beach at Transect D was about 18 m narrower than in January 2009, representing one of the most retreated conditions since the start of monitoring (Figure 10a). South of the coastal defences (Transect E) the beach was relatively stable in the period 2016–2018 despite being slightly retreated from its position in 07-Jan-2009 (Figure 11a). The largest changes in beach levels (2.5 m, Figure 11b) were due to the mobility of gravel ridges.

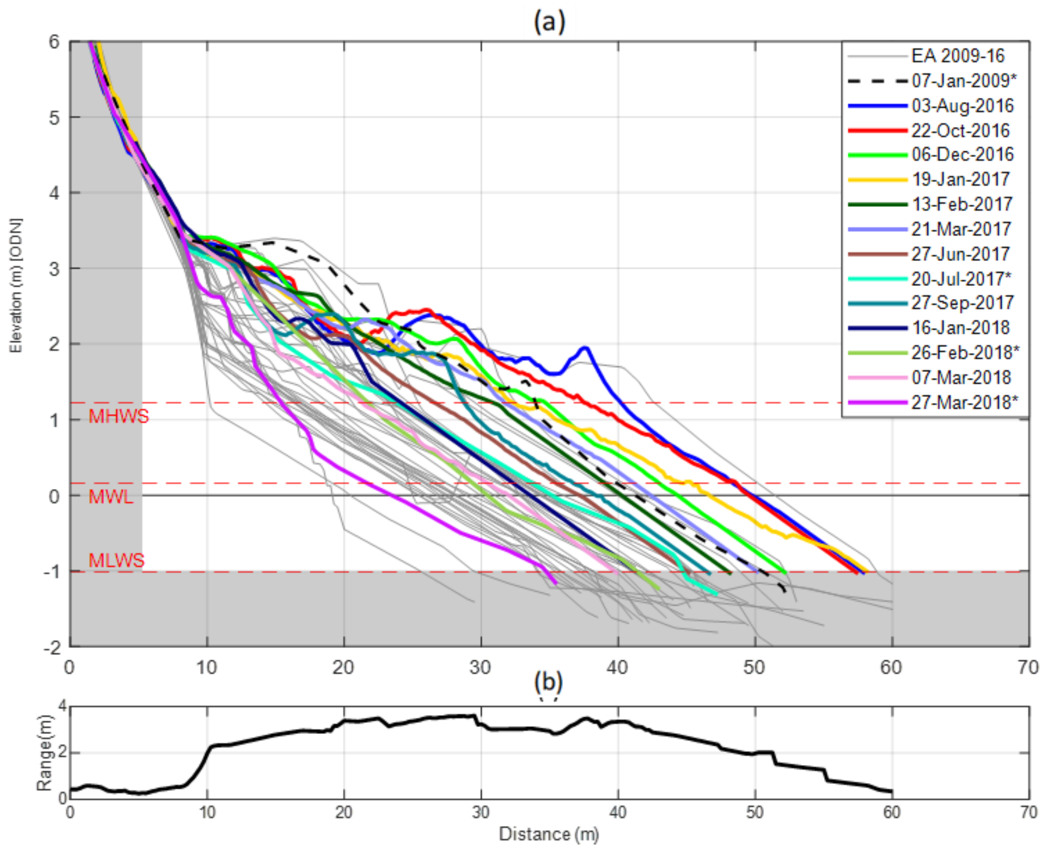

Figure 10. Beach profiles measured along Transect D between January 2009 and March 2018 (a) and maximum changes in elevation along the cross-shore profile (b). For reference, the initial profile (07-Jan-2009) measured by the Environment Agency is shown as a dashed line, while all other EA profiles are shown in grey.

Multiple gravel ridges occurred above MHWS along Transect D, and they seem to influence changes in morphology as observed in Transect A. The gravel ridge closest to the waterline controls changes further up the beach. Multiple gravel ridges develop during the summer, with the topography becoming flatter across the winter. During summer (26-Jul-2016 to 3-Aug-2016), the gravel ridge closest to the waterline migrated up the beach, becoming wider and less defined until it coalesced with other ridges in late autumn/early winter. In the absence of a gravel ridge, the profile below MHWS eroded, while changes above MHWS were negligible. The pattern of ridge formation in the summer and migration and fading in the autumn/early winter seemed to repeat in 2017. Along Transect E, ridges remained well-formed, showing little change during the summer and persisting during the winter, albeit much less developed. It is worth noting that the beach below MHWS retreated in early autumn and showed little change or slight accretion during the winter.

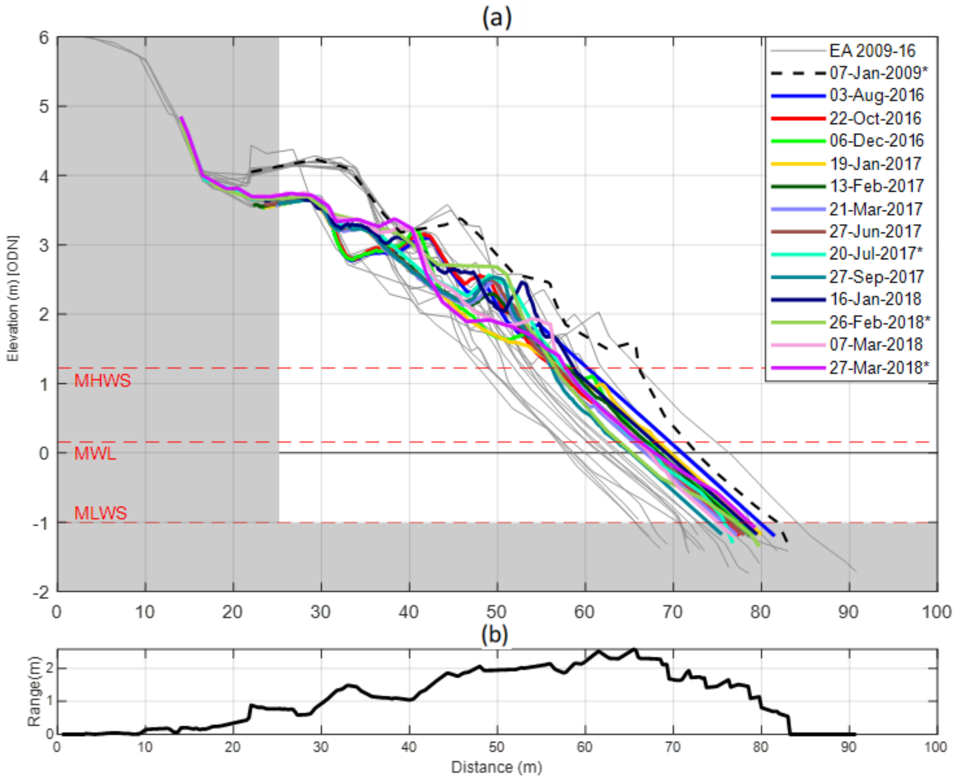

Figure 11. Beach profiles measured along Transect E between January 2009 and March 2018 (a) and maximum changes in elevation along the cross-shore profile (b). For reference, the initial profile (07-Jan-2009) measured by the Environment Agency is shown as a dashed line, while all other EA profiles are shown in grey.

4. CHANGES IN THE NEARSHORE

Changes in bathymetry indicate areas where sediment is eroded (increase in depth) or deposited (areas become shallower). Two bathymetric (multibeam) surveys obtained in July 2014 (Figure 12a) and January/February 2017 (Figure 12b) were analysed to identify where magnitudes of change are largest (Figure 12c). The multibeam survey obtained in 2017 was concomitant with radar data collection and served to establish the accuracy of the depth derived from radar data. Once the radar-derived bathymetry was validated, an extensive data quality control procedure was established to identify the data suitable for the production of bathymetric maps. About 53 ‘blocks’ of data met the quality control criteria; the longest data gap between ‘data blocks’ was 80 days. However, analysis is only warranted when bathymetric changes are greater than the error inherent to the method.

Multibeam surveys are more precise than radar-derived bathymetry, but they are expensive and thus obtained infrequently and limited to areas of high interest. Although radar-derived bathymetry is less precise (error within ±0.5 m when quality control conditions are met, see Appendix C), it enables an assessment of changes over larger nearshore areas at frequencies that are prohibitively expensive by other means.

The multibeam surveys show clearly the Coralline Crag ridges extending in a SW-NE direction across the seabed, and the presence of mobile large-scale bedforms, likely to be sand waves (Figure 12a, b). In 2014, these bedform features occurred in the nearshore and offshore with varying spacing and orientation (Figure 12a). In 2017, they are evident only offshore, where their movement seem to be controlled by the southernmost Coralline Crag ridge (Figure 12b). An oblique nearshore bar extending from the ness in a northwest-southeast direction is a prominent feature that appears more developed in 2014 than in 2017.

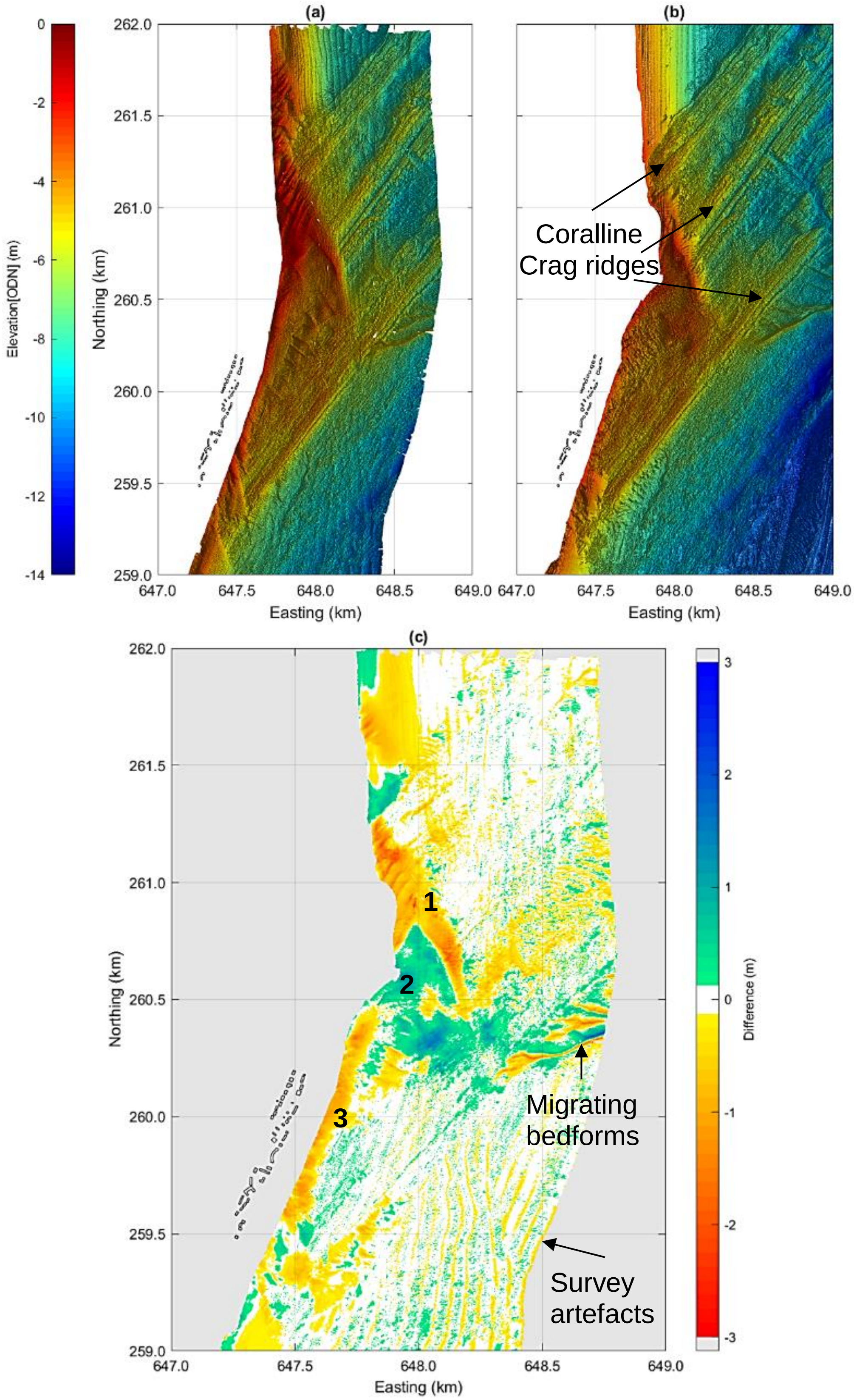

Figure 12. Bathymetry obtained from two multibeam surveys undertaken by (A) the EA in June 2014 and (B) the Maritime Coastal Authority in January 2017. (C) Difference in the depths recorded between the 2014 and 2017 surveys, negative values indicate an increase in depth (usually due to sediment loss) and positive values indicate a reduction in depth (usually due to sediment gain). Areas in white represent changes within ±0.125 m.

It was possible to identify three areas (numbered sequentially from north to south) where changes in bathymetry between the two surveys were large (Figure 12c). In Area 1, there was an increase in depth, of up to 2 m, due to erosion of the nearshore oblique bar. In Area 2, a reduction in depth of up to 2 m was observed to the south and shoreward of Area 1. The erosion in Area 1 and accretion in Area 2 seem to result from a clockwise rotation of the oblique bar. In Area 3, the depth increased up to 1.5 m closer to shore along most of the southern half of the survey area, including the beach frontage of Thorpeness. Offshore of Area 2, bands of erosion and accretion alternate, suggesting a north-easterly migration of large bedforms (2 m high, 20-50 m wide). The apparent bands of erosion aligned approximately north-south across the survey area are believed to be artefacts of the surveying method, as they match the trajectory of the vessel in 2014.

X-band radar data enabled analysis of bathymetric changes at time-scales varying from 23 days to six months (or longer). Examples of the bathymetric maps derived from radar data are shown in Figure 13. Largest changes were observed at the same three areas identified in the analysis of the multibeam surveys. However, it became clear that the magnitudes of changes observed to occur over the 2.5 years between surveys, can occur at much shorter intervals. Changes in bathymetry of up to +2 m in Area 1 occurred within four months between 11-Oct-2015 (Figure 13a) and 06-Feb-2016 (Figure 13b), magnitudes similar to the erosion in Area 1 and deposition in Area 2 recorded between June 2014 and January 2017.

The largest changes in volume estimated based on radar data occurred between 11-Oct-2015 and 6-Feb-2016, when an overall net accumulation of 74,000 m^3 of sediment is estimated across the study area, showing deposition in Area 1 (118,400 m^3) and erosion (37,736 m^3) in Areas 2 and 3 (Table 5). Volume changes in Areas 1 and 2 seem to be reversed, when one shows net accretion, the other shows net erosion, particularly at periods of analysis longer than 4 months. Net volume changes can be considerable 29,735 m^3) even over short periods (e.g. 23 days), as observed between 21-Jan-2017 and 13-Feb-2017 (Table 3). As suggested by Burningham and French (2017), underlying geology seems to play a role in controlling nearshore dynamics. The position of the ness and the adjacent nearshore oblique bar and the associated areas of largest changes (Areas 1 and 2) are likely to be controlled by the presence and orientation of the Coralline Crag ridges.

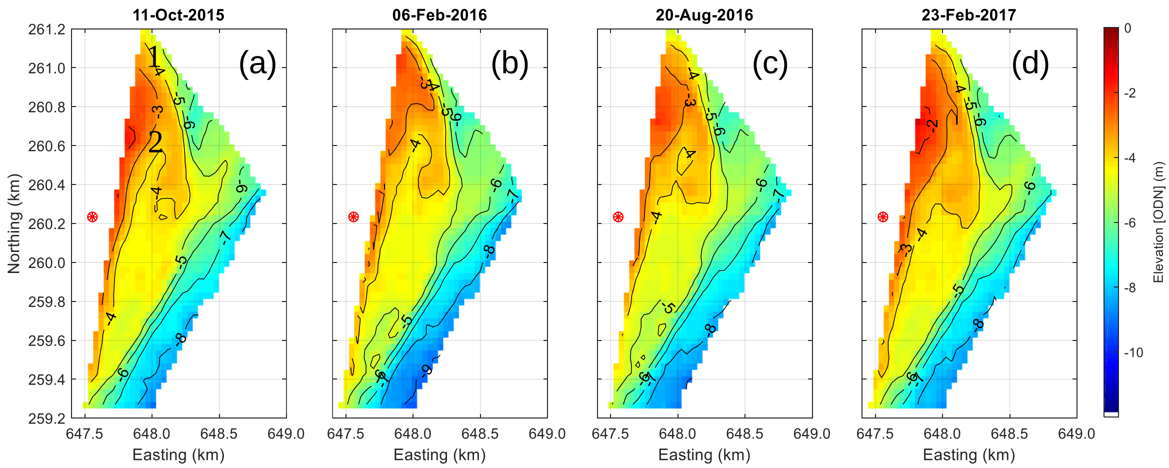

Figure 13. Examples of X-Band radar-derived bathymetry at four selected dates: (a) 11-Oct-2015, (b) 06-Feb-2016, (c) 20-Aug-2016, and (d) 23-Feb-2017. The radar position is shown as a red circle.

Table 5. Volume changes over periods of approximately 4 to 6.5 months within the three areas where largest changes were observed.

		Area 1		Area 2		Area 3	
Date 1	Date 2	Area (m^2)	Volume (m^3)	Area (m^2)	Volume (m^3)	Area (m^2)	Volume (m^3)
11-Oct-2015	06-Feb-2016	118400	+112196	60800	-26063	19200	-11653
06-Feb-2016	20-Aug-2016	48000	-36453	25600	+16818	1600	-1068
20-Aug-2016	23-Feb-2017	92800	-71343	46400	+35241	0	0

5. EFFECTS OF THE BIMODAL WAVE DIRECTION

The radar data allowed, for the first time, an assessment of how changes in dominant wave direction affect the nearshore bathymetry. Here, changes in nearshore bathymetry occurring during periods of 4-6 months are analysed in relation to the respective offshore wave conditions and contrasted with beach changes (recorded at the best matching dates). Beach changes are represented as the changes in beach width at MHWS along the existing transects monitored by the EA in the study area (TN001 to TN036).

The changes in the nearshore recorded between 11-Oct-2015 and 6-Feb-2016 (see Section 4) seems to be more or less in phase with changes observed at the adjacent beach (note the difference in dates). Accretion was observed in nearshore Area 1 and the beach width increased up to 37 m around the ness (Figure 14a). Erosion dominated in nearshore Area 2 with the adjacent beach either narrowing or, at best, remaining stable. North of the radar, there was a retreat of 8.5 m in the position of the cliff toe. Further south, some erosion was observed in nearshore Area 3, but the adjacent beach remained stable or accreted, with erosion observed only in the southernmost transects (Figure 14a).

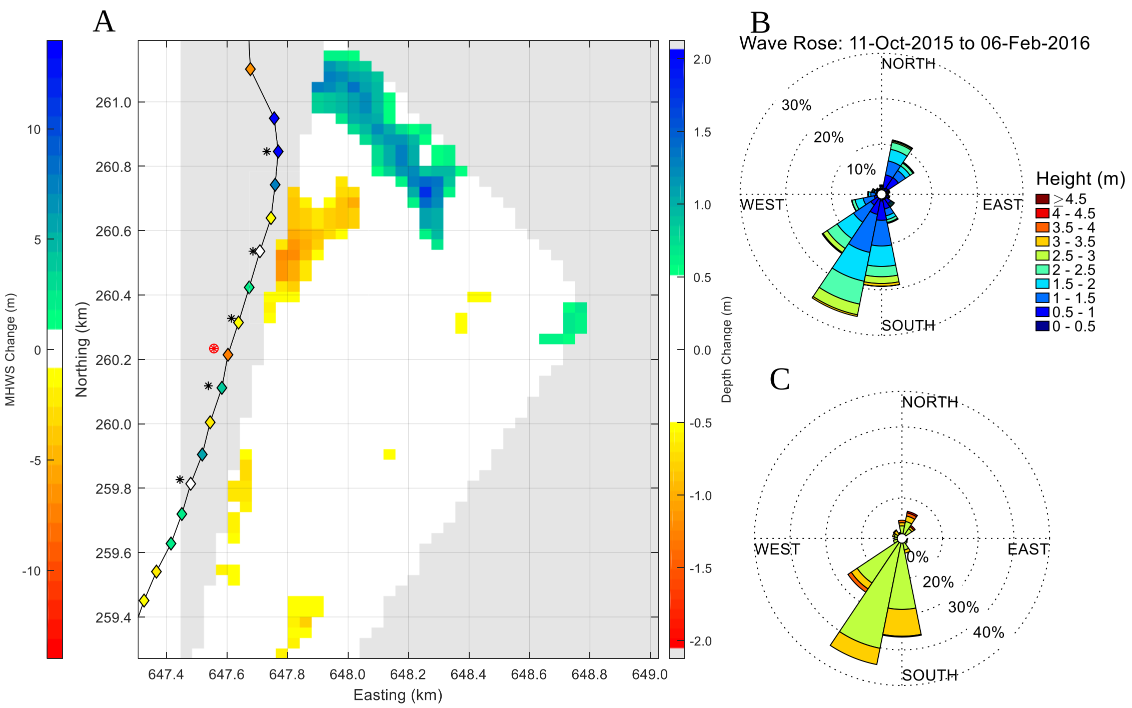

Figure 14. (A) Changes in radar-derived bathymetry between 11-Oct-2015 and 06-Feb-2016. The black line indicates the MHWS on 02-Feb-2016 and markers indicate changes in beach width at MHWS between 05-Aug-2015 and 02-Feb-2016. Wave roses for the period 11-Oct-2015 and 06-Feb-2016 are shown for (B) all waves and for (C) H_s>2.5 m only.

Southerly waves dominated during this period (Figure 14b), particularly the highest (Figure 14c), as 81% of waves with Hs >2.5 m approached from a southerly direction. These waves seem to favour nearshore erosion in the south and accretion in the north. It is possible that these wave conditions move sediment from Areas 2 and 3 shoreward and to the north, contributing to the accretion in Area 3 and at the ness. However, there was an estimated net gain of more than 74,000 m^3, suggesting a contribution from areas unaccounted for due to small magnitudes of changes (within the error band of the radar) or an external input of sediment.

Between February and August 2016, gross and net (18,567 m^3) volume changes in the nearshore were much lower (Figure 15a) than in the period described above. Bathymetric changes exceeding 0.5 m occurred over a smaller area, with erosion now dominating in Area 1 (up to -1.15 m change in depth) and accretion (up to +0.89 m change in depth) in Area 2 (Figure 15a). There was a more balanced proportion of waves approaching from a northerly and southerly direction (Figure 15b), 48% and 42%, respectively, but the highest waves were dominantly from the S-SW (Figure 15c). In the northern sector, beach changes follow the pattern of nearshore changes, while beach erosion was observed north of the radar and beach accretion to the south (Figure 15a). Northerly waves seem to erode the nearshore oblique bar (Area 1) and, further south, promote beach accretion and nearshore stability.

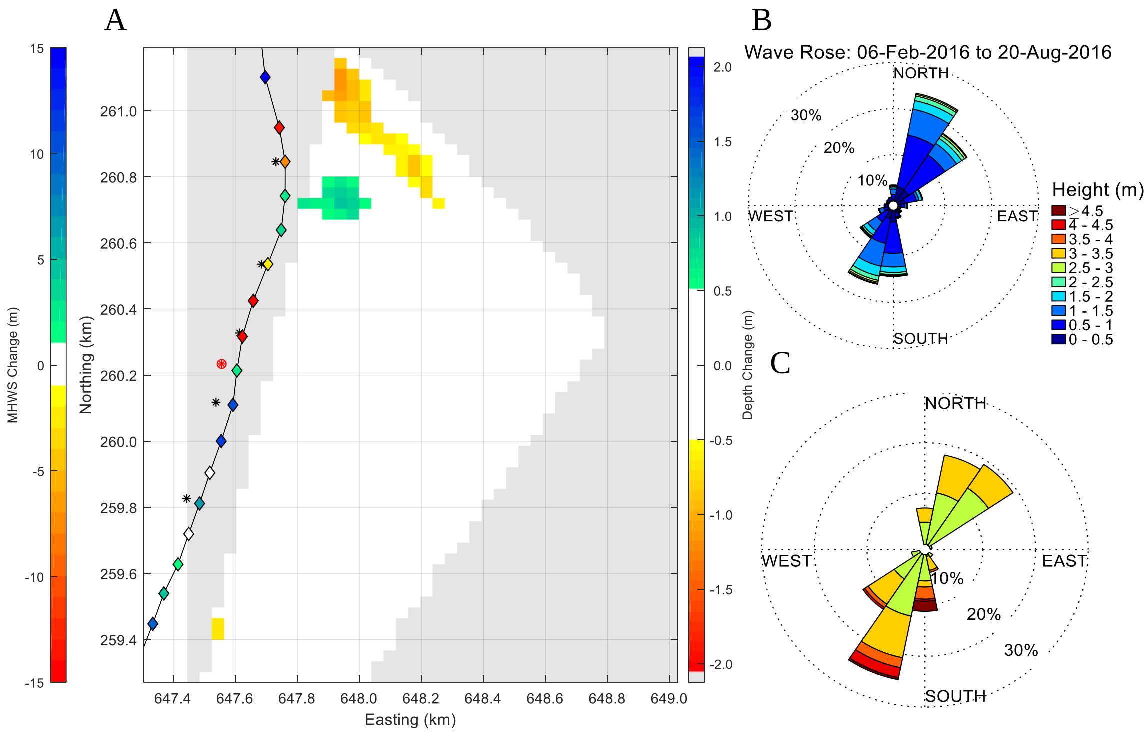

Figure 15. (A) Changes in radar-derived bathymetry between 06-Feb-2016 and 20-Aug-2016. The black line indicates the MHWS on 27-Jul-2016 and markers indicate changes in beach width at MHWS between 02-Feb-2016 and 27-Jul-2016 Wave roses for the period 06-Feb-2016 and 20-Aug-2016 are shown for (B) all waves and for (C) H_s>2.5 m only.

Between August 2016 and February 2017, erosion intensified in nearshore Area 1 and accretion in Area 2 (Figure 16a), resulting in a net loss of sediment over 36,102 m^3. Beach retreat (up to 16 m) dominated across the study, although magnitudes were much lower in the southern sector. This period shows a relative balance between northerly (41%) and southerly (43%) waves (Figure 16b). The highest waves are dominantly from a northerly direction (Figure 16c), which seem to intensify erosion, particularly in the northern sector.

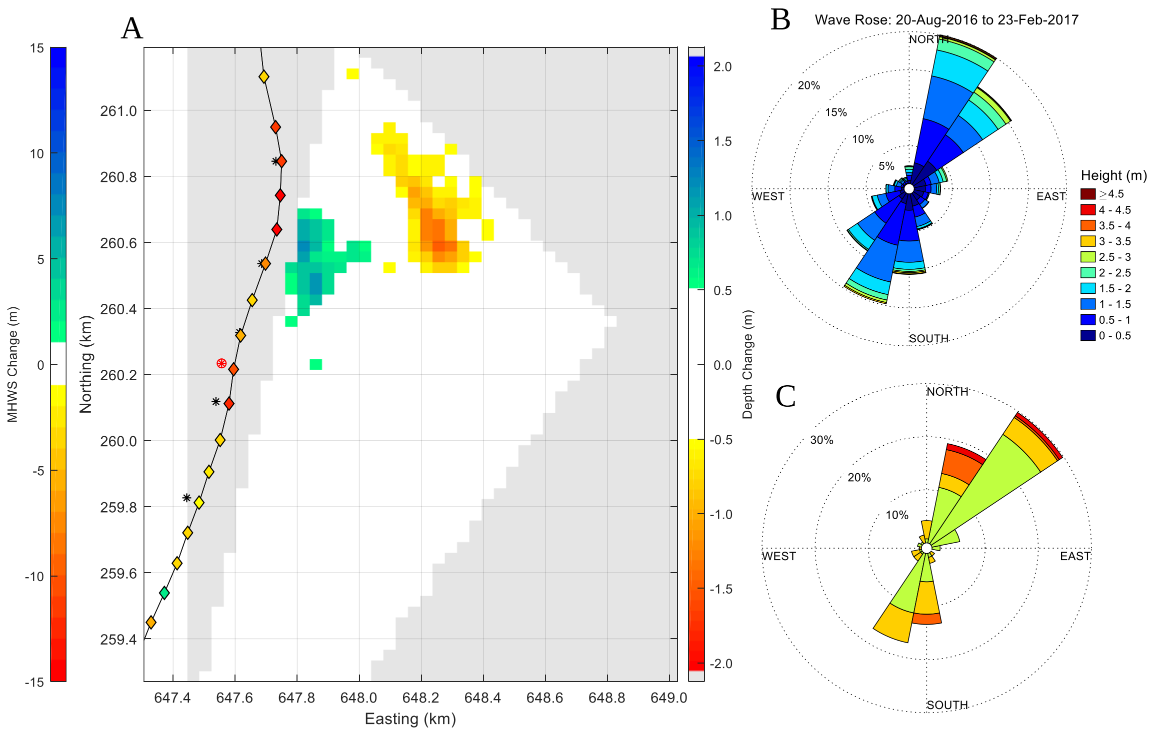

Figure 16. (A) Changes in radar-derived bathymetry between 20-Aug-2016 and 23-Feb-2017. The black line indicates the MHWS position on 06-Mar-2017 and markers indicate changes in beach width at MHWS between 27-Jul-2016 and 06-Mar-2017. Wave roses for the period 20-Aug-2016 and 23-Feb-2017 are shown for all waves (B) and for H_S>2.5 m only (C).

The erosion and accretion patterns in the nearshore are neither seasonal nor regularly spaced in time. For example, Area 1 appears in an 'accreted state' in the summer (June/July 2014) and in the winter (February 2016), with the oblique bar forming over 4-6 months but taking longer to be eroded (12 months). This pattern is determined primarily by the dominant wave direction and length of time high waves occur from a southerly or northerly direction. In the period of analysis, no clear seasonal signal was found on these two variables. It is possible that this variability may be controlled by wider atmospheric circulation patterns, such as the effects related to the North Atlantic Oscillation (NAO), but confirming this requires further investigation.

6. SEDIMENT TRANSPORT

The effects of the dominant wave direction on beach changes are also influenced by the state of the nearshore when wave conditions change. Numerical modelling simulations indicate that the alongshore variability in beach response may be due to variations in the flux of sediment transport determined by how waves interact with nearshore features. Differences arise both due to changes in the dominant wave direction and whether parts of the nearshore are more or less depleted of sediment. Certain conditions may affect the direction of longshore transport locally, creating an area of focused erosion or accretion, due to divergence or convergence of sediment transport, respectively.

The occurrence of beach erosion or accretion at any particular coastal stretch is determined by the sediment budget, which is the difference between how much sediment is supplied and removed within a specific period of time. Deposition occurs when there is a surplus of sediment (more sediment is supplied than removed) and erosion occurs when there is a sediment deficit (more sediment is removed than supplied). Sediment can be transported parallel to the coast within the surf zone (longshore transport) or in a cross-shore direction (from dunes/cliff to the beach and nearshore or vice-versa).

A numerical model was used for the study area to establish how a changing nearshore interacts with the bimodal wave climate and how this affects the wave energy arriving at the shoreline. Two coastal area models (CAM) were built to represent different nearshore conditions: CAM1 with the Jul-2014 bathymetry and CAM2 with the Jan-2017 bathymetry. The models were validated and used to calculate the longshore sediment transport (LST) flux using ten years of wave data (January 2007 to December 2017). The LST flux at 123 locations between Aldeburgh and Thorpeness (matching every EA monitoring profile) was calculated using Equation 1 (Van Rijn 2014):

$$Q = 0.00018\rho_s g^{0.5}(tan\beta)^{0.4}(D_{50})^{-0.6}(H_{sb})^{3.1}(sin(2\theta)) \qquad \text{(Equation 1)}$$

where Q is the LST flux ($m^3\ s^{-1}$), ρ_s is the sediment density (assumed to be 2650 kg m^{-3} for the sand fraction and 1500 kg m^{-3} for gravel, g is the acceleration due to gravity (9.8 m s^{-1}), $tan\beta$ is the beach slope, D_{50} is the median grain size (calculated for both the sand and gravel fractions, 0.3 mm and 14 mm, respectively), H_{sb} is the significant wave height at the breaking point and θ is the wave angle relative to the shoreline. LST calculations considered three time-frames: (1) the average annual flux over the 10-year period; (2) winter periods dominated by southerly and northerly waves; and (3) storm events dominated by southerly and northerly waves.

Calculations of annual flux suggest that the sediment grain size influences only the volume of LST, with sand transport (Figure 17a) being one order of magnitude greater than gravel (Figure 17b), as relative changes alongshore remain the same. The highest annual LST flux is in the order of 32,000 $m^3\ a^{-1}$ of sand and 3,500 $m^3\ a^{-1}$ of gravel moving northward along the southern flank of the ness for CAM2 (2017) nearshore conditions. The highest flux is at the same location but slightly reduced for CAM1 (2014), showing around 28,000 $m^3\ a^{-1}$ of sand transport (Figure 17a) and 3,000 $m^3\ a^{-1}$ of gravel (Figure 17b). At this temporal scale, there is a clear convergence of sediment at the ness for both CAM conditions, as the LST flux is southward north of the ness and northward south of the ness. Therefore, over the 10 years, conditions were favourable for the maintenance and accretion of the ness. At Thorpeness, the annual LST flux is dominantly northward and a localised sediment deficit may be explained at the location where more sediment is transported north than arrives from the south.

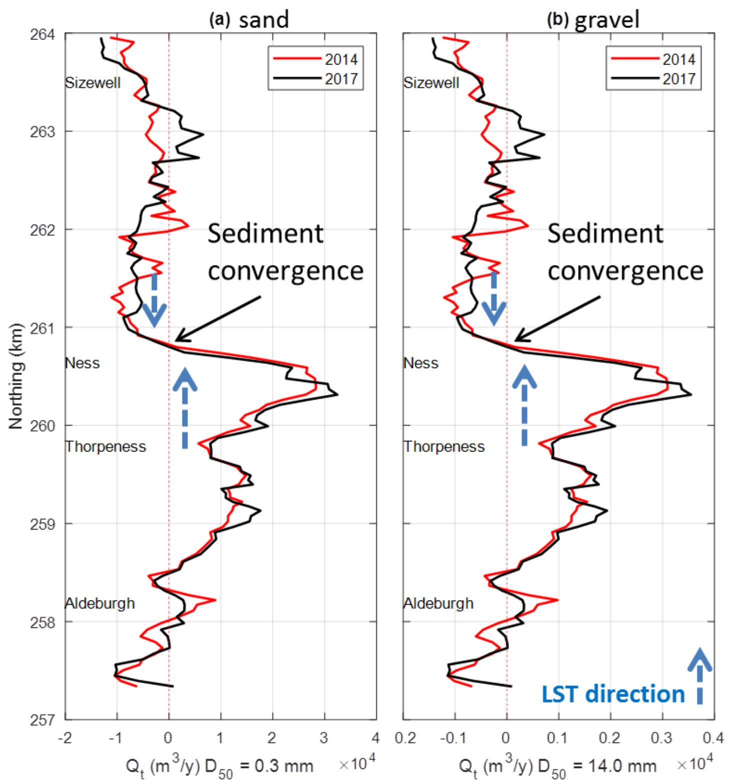

Figure 17. Mean annual LST flux calculated based on 10 years of wave data for nearshore conditions in 2014 and 2017 and (a) the average D50 of the sand fraction (0.3 mm) and (b) the average D50 of the gravel fraction (14.0 mm). Negative values indicate a southward flux and positive values a northward flux.

The nearshore bathymetry affects the annual LST flux at some locations, particularly north of the ness. There, LST flux is dominantly south and generally lower than 10,000 m^3 a^{-1} of sand (Figure 17a) and 1,000 m^3 a^{-1} of gravel (Figure 17b). Northward LST is observed along short coastal stretches, located further north and more pronounced for CAM 2 (2017), which indicates that the direction of net LST can reverse depending on the nearshore conditions.

Investigating the mean annual LST over a number of years provides an indication on the net volume of sediment movement, relative differences along the coast and longer-term trends. However, it does not elucidate what happens in shorter periods and in response to specific conditions. Previous studies have identified that magnitudes and direction of LST can vary considerably in the study area according to wave direction and energy (Burningham and French 2016). To better understand these variations, LST calculations were undertaken for periods dominated by northerly and southerly waves at two time-frames: over the winter months (Figure 18) and at the time of the highest wave from the NNE and the SSW recorded in the 10-year dataset (Figure 19).

As expected, the LST flux is primarily to the south in the winter dominated by northerly waves, except around the southern side of the ness, where the LST is to the north (Figure 18a). Therefore, these conditions create a convergence of sediment at the ness and a divergence of sediment north of Thorpeness, where cliff retreat is most intense (around Transect C). The highest northward sand transport reaches 10,000 m^3 south of the ness while the southward transport is usually <10,000 m^3, except south of Thorpeness towards Aldeburgh.

North of the ness, the LST continues southward even in winter conditions dominated by southerly waves (Figure 18b). However, south of the ness to around Aldeburgh, the LST flux is northward. Therefore, the net LST direction reverses along Thorpeness and the position of sediment divergence shifts southward according to the dominant wave direction. Magnitudes of LST tend to be smaller in the winter dominated by southerly waves, reaching a maximum of 7,500 m^3 south of the ness and <5000 m^3 elsewhere.

The nearshore conditions seem to have a localised effect on the magnitude of LST, which can differ up to 5,000 m^3 when northerly waves dominate and less than 2,500 m^3 when southerly waves dominate. LST can be higher or lower in 2014 depending on the site. Another effect, observed only in the winter dominated by southerly waves, is the shift in the position of the sediment convergence, which is slightly to the north in 2014 than its position in 2017 (Figure 18b).

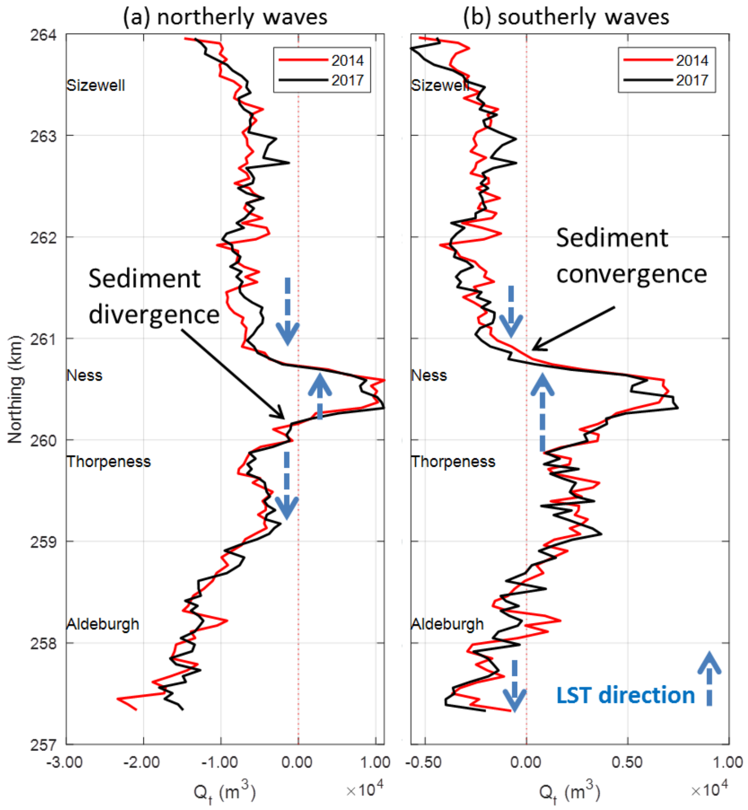

Figure 18. LST flux of the sand fraction (D50 = 0.3 mm) calculated for nearshore conditions in 2014 and 2017 under winter conditions dominated by (a) northerly waves (01-Dec-2009 to 28-Feb-2010) and (b) southerly waves (01-Dec-2015 to 28-Feb-2016). Negative values indicate a southward flux and positive values a northward flux.

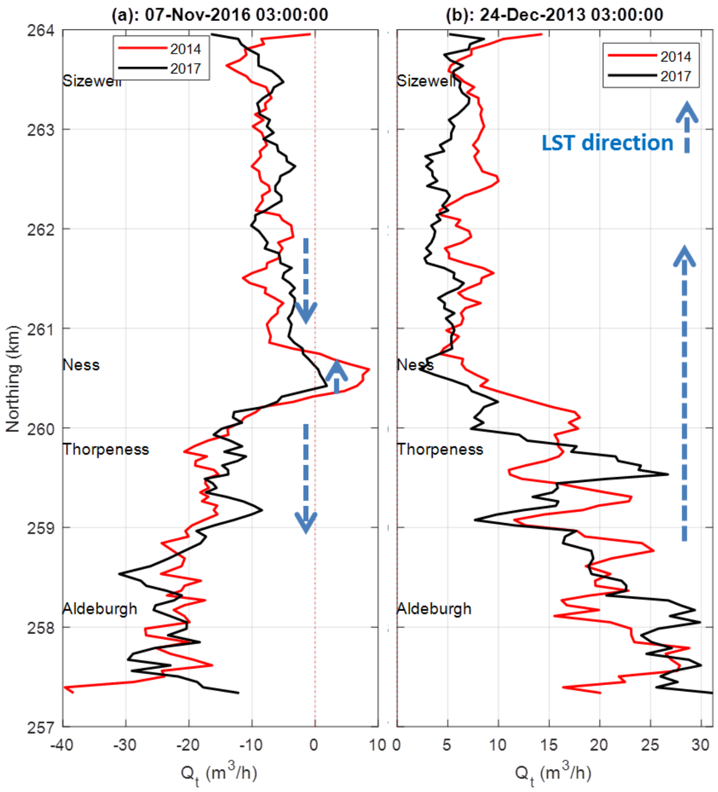

Figure 19. LST flux of the sand fraction (D_{50}=0.3 mm) calculated for nearshore conditions in 2014 and 2017 under the highest wave recorded within the 10-yr dataset from (a) a northerly direction (07-Nov-2016, Hs =4.29, DirP =22, Tp =9.04) and (b) a southerly direction (24-Dec-2014, Hs =4.53, DirP =196, Tp =7.42). Negative values indicate a southward flux and positive values a northward flux.

Localised reversals in LST direction are apparent around Aldeburgh, at different locations in CAM 1 and CAM 2, making the position of the sediment divergence less obvious.

The effects of nearshore bathymetry on LST are more prominent at short time-frames when waves are solely from one direction. As an example, Figure 19 shows the LST flux estimated for the highest northerly (07-Nov-2016) and southerly (24-Dec-2013) waves within the 10-year dataset. As observed at other time-frames, the LST flux is reduced along the northern sector (<10 m^3/h), increasing south of the ness to 30 m^3/h around Aldeburgh. LST flux tends to be higher (more than double in some cases) under 2014 conditions, with some exceptions, including around Aldeburgh for both wave directions and at Thorpeness during high southerly waves.

High northerly waves drive the LST southwards, except at the ness, particularly under 2014 nearshore conditions (Figure 19a). High southerly waves drive the LST northwards (Figure 19b). Differences in the magnitude and direction of LST flux between Thorpeness and the ness provide a plausible explanation for the observed alongshore variability in beach response identified in the profile analysis. The LST modelling has shown that most conditions, irrespective of bathymetric changes, result in sediment convergence at the ness. However, apart from temporary erosion and accretion phases, the sediment volume of the ness remains relatively constant. This implies that there must be exchanges of sediment between the ness and the nearshore as suggested by McCave (1978) and Carr (1981). The observed growth and erosion phases of the nearshore oblique bar may be a result from sediment exchange to and from the ness. Further investigation would be required to confirm these links and any implications to the maintenance or movement of the Sizewell Bank.

The results presented above indicate that the sediment volume at the ness is more or less stable through time due to a convergence of sediment, with the largest volumes supplied through sediment moving northward. Therefore, it is possible that small-scale extraction of gravel from the mobile part of the ness (below MHWS) to recharge the beach at Thorpeness may not have a detrimental impact in the dynamic stability of the ness. The chance of impact is reduced because, after some time, the material is likely to return to the ness naturally due to LST. However, the timing and scale of these operations must be carefully planned to ensure that the amount of material removed can be replaced naturally at time-scales that can offer the coastal protection required at Thorpeness without having a detrimental impact elsewhere. To avoid unintended impacts, the ‘tipping point’ or threshold for the removal of sediment needs to be identified, possibly with the help of targeted modelling simulations.

7. WILL AN INCREASE IN THE PROPORTION OF SAND RESULT IN ENHANCED EROSION?

It is well-known that beach stability (or erosion) is determined by the energy of the dynamic processes (such as waves and currents) and the characteristics of the beach material. In very simple terms, erosion occurs when the energy is enough to re-suspend and transport particles and, generally, more energy is required to erode larger/denser particles. Consequently, under the same energy conditions, gravel beaches tend to be more stable than sandy beaches. However, complications arise when beaches are formed by a mixture of gravel and sand; mainly as a result of differences in density between sand and gravel and changes in sediment porosity (the empty spaces between the sand and gravel particles).

The porosity determines how much water infiltration can happen when waves come up the beach. Infiltration (or more technically the hydraulic conductivity) helps dissipating wave energy and reduces the chance of material being removed by the backwash (the water movement back to the sea due to gravity). Pure gravel shows the highest hydraulic conductivity as the water infiltrates the pores more easily, dissipating wave energy more effectively. In mixed sand and gravel beaches, sand grains occupy the spaces between the gravel, causing a reduction in porosity. Previous studies have identified that a critical threshold occurs when the proportion of sand exceeds 35-40% (Mason and Coates 2001; She et al. 2006; Horn and Walton 2007), as the hydraulic conductivity will be reduced in a way that will effectively be the same as pure sand. In such conditions, there is less dissipation of wave energy and erosion may be enhanced.

This critical threshold affecting the hydraulic conductivity of mixed sand and gravel was primarily identified in laboratory tests and beach recharge material, where proportions of sand and gravel can be easily defined. Defining the proportions of sand and gravel in natural mixed beaches is not as simple. These proportions vary in time and space (Figure 20), between the beach surface (the top few centimetres) and subsurface (into the sediment layer) and across the profile, often being more sandy in intertidal areas than above MHWS. To assess whether the critical threshold is valid for natural beaches, it is difficult to determine where, when and how the proportion of sand and gravel should be measured. To our knowledge, this research was the first ever attempting to verify whether there is a relationship between the proportion of sand and erosion in a natural mixed beach. A major challenge was to determine where to obtain the measurements and how to estimate the proportion of sand and gravel without having to remove and transport to the laboratory many kilos of beach material.

Determining the proportion of sand and gravel is not a complex task, but sampling can be logistically difficult due to the size/weight of samples and the number of samples that need to be collected if the site shows large variations in space and time. Some authors suggest that large samples, composed of more than 100 particles for each 0.25 phi fraction (about 400 particles for each grain size class), are required to fully quantify the gravel size distribution (Gale and Hoare 1992). Others argue that several smaller samples would provide a better representation of spatial and temporal variations in sediment size (Dornbusch et al. 2005; Horn and Walton 2007). Or simply that the research aims dictate the sampling required (Dunkerley 1994).

Traditional methods to determine the proportion of sand and gravel require large samples (3-5 kg) to be taken at each point along the beach profile where changes in topography and grain size are observed. Between Thorpeness and the ness, variance in the distribution of gravel and sand is a key characteristic; between four and nine samples would be required at each beach transect. These sampling would then be repeated in every fieldwork to assess temporal changes. Such approach can be prohibitive depending on the size of the study area, its variability and ease of access. The five beach transects monitored in this research are distributed along 2 km of shoreline, most of which accessible only by foot. Following this sampling method would involve collecting about 30-40 samples or a total of 90-200 kg during each field campaign and time-consuming work in the laboratory. Therefore, an alternative and more feasible method was devised to quantify the proportion of sand and gravel and how it varies in space and time, combining in situ measurements, digital image analysis and sediment sampling.

Figure 20. Examples of variability in the distribution of sand and gravel in the area of Transect C, where bands of gravel can form (a) perpendicular or (b) parallel to the waterline, often having (c) gravel dominating above MHWS and (d) sand dominating below MWL.

7.1. A COST-EFFECTIVE SAMPLING STRATEGY

Along each beach transect, the sampling points were defined where major changes in morphology or sediment size were observed. Typically, measurements and/or samples were taken at four to nine points along each transect: at the upper beach (cliff toe/base of coastal defences); along the berm; berm overwash; intertidal terrace and on/between gravel patches/ridges). The following measurements or samples were obtained at each point:

a) Thickness of gravel (where present at surface) – by digging a small trench with a garden trowel until sand was the dominant grain size allowed the thickness of the gravel layer to be measured using a ruler. For practical reasons, if sand was not found within the top 35 cm, the gravel layer was simply assumed to be thicker than 35 cm.

b) A photograph of the sediment surface was taken (only if gravel was present) following a systematic procedure - the proportion of the sand and gravel at surface and the size distribution of gravel were determined through semi-automated digital image analyses using a simple grid-count method (Hey and Thorne 1983; Yuzyk and Winkler 1991). The images were overlain with a 10 x 10 digital grid (Bunte and Abt 2001), at each intersection (100 points), the size of the nearest particle was estimated as the length of its intermediate axis using the Jann5s Measure Tool function (v2.01) in Matlab. A correction factor (*1.07) was applied to account for differences between measurements obtained using a manual calliper and the image analysis (Adams 1979). The proportion of sand and gravel at surface was determined by identifying whether sand or gravel was present at each grid intersection and then calculating their relative percentage.

c) A sediment sample (only if sand was present) was collected and taken to the laboratory for the particle size distribution of fraction smaller than gravel (< 2 mm) to be measured by laser diffraction in a Mastersizer 3000.

On one occasion (27-Sep-2017), bulk samples were collected from the intertidal zone of Transects B and D at three levels: at surface, 2 cm below the surface and 10 cm below the surface. The proportions of sand and gravel (by weight) were measured for each sample. The average proportion of sand of all subsurface samples (34%) was assumed to be a close approximation of the sediment mixture found below the gravel layer (or below the surface if gravel is not present) across the study area.

The data described above enabled estimating: the proportion of sand at surface and at depth; the grain size distribution of gravel; and the grain size distribution of sand. With this information and making some approximations, it was possible to estimate the proportion of sand at different parts of the beach profile along the five transects on each fieldwork date. These data were then used to assess whether there was any evidence that a higher proportion of sand would lead to greater sediment mobility (erosion). The approximations made in the calculations include:

- the proportion of sand and gravel at each sampling point was extended to the midpoint towards the next sampling point, where the characteristics of the latter would then be applied (Figure 21);
- the proportion of sand and gravel at surface was assumed to be unchanged at depth (subsurface), except where a gravel layer with thickness <35 cm was found;
- below the gravel layer, the sediment was assumed to be 34% sand and 66% gravel;
- the calculations of the proportion of sand within each beach compartment (between and above the MLWS, MWL and MHWS) were confined to a layer of 40 cm to limit the uncertainties related to the method.

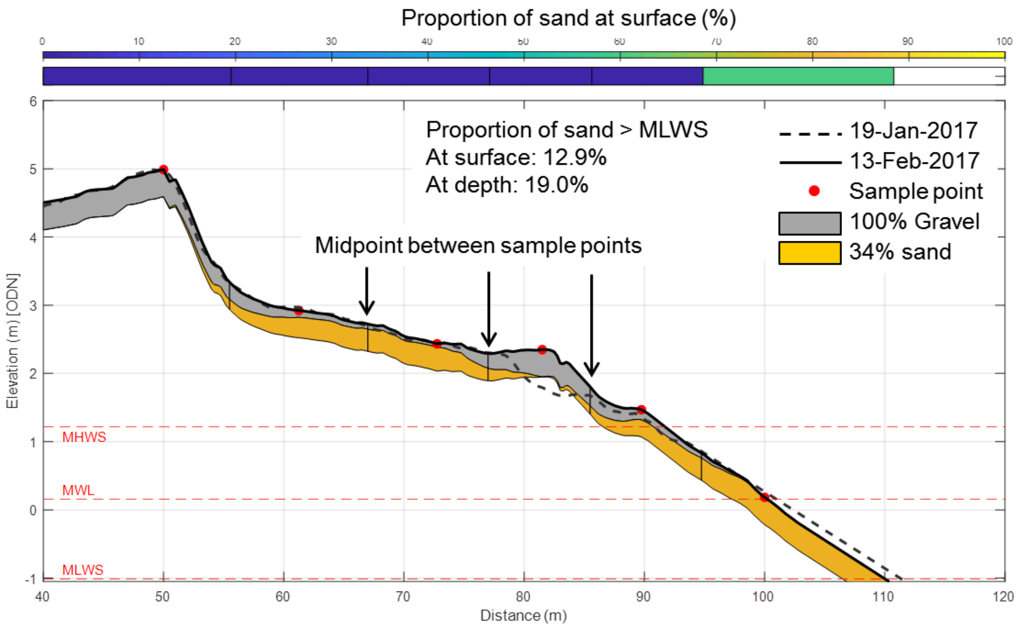

Figure 21. Representation of the sediment data along Transect A, showing: the topography on 19-Jan-2017 and in the previous survey on 13-Feb-2017; the distribution of the gravel and the mixed sediment layer (34% sand) within to top 40 cm and along the profile; and at the top, the proportion of sand at surface (the scale shows blue as 0% and yellow as 100%).

7.2. Complexity of Results

A comprehensive set of statistical analyses were used to test whether a significant relationship exists between the proportion of sand (at depth and at surface) within each beach compartment along the five transects and respective proxies of coastal change. Proxies of coastal change included: beach width at MLWS, MWL and MHWS, cross-sectional area at each beach compartment and their changes per day between surveys. The analysis was conducted first for all data and then for individual transects.

The strongest significant correlations were found between the proportion of sand at depth and beach width at MHWS (rho=-0.68, n=45, p<0.000) and also the cross-section area above MHWS (rho=-0.512, n=45, p<0.000). In all cases, negative correlations were found, which indicates an association between higher proportions of sand above MHWS and smaller cross-sectional area and narrower beach width at MHWS. No significant correlation was found for parameters measured below MHWS.

The analyses of data from individual transects show that the relationship between beach changes and proportion of sand differ between transects. These results are based on a relatively small number of measurements and should be considered with caution. Significant relationships were found for changes measured at Transects A, C and E only. Interestingly, positive correlations were found for measurements at Transect A, while negative correlations were found for Transects C and E (Figure 22). It means that an increase in the proportion of sand is associated with beach accretion at Transect A and erosion at Transects C and E. Most of the significant correlations were found with the proportion of sand at depth.

At Transect A, relationships were observed between the proportion of sand at depth and changes in beach width (at MLWS, MWL and MHWS) and profile area for beach compartments below MHWS only. The strongest correlations were found between the percentage of sand in the intertidal area (MLWS-MHWS) and changes per day in both beach width at MWL (Figure 22a) and cross-sectional area within MLWS-MHWS (Figure 22b). The proportion of sand was found to be lower than 35% in most cases and associated with erosion rates, while proportions higher than 35% were associated with accretion.

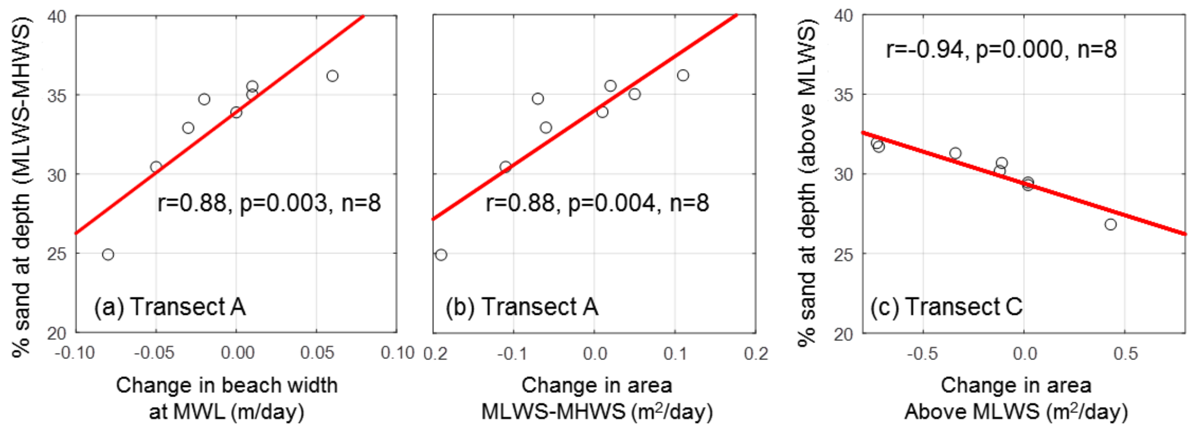

Figure 22. Scatter plots showing linear regression line and results of Pearson correlation coefficient (r), level of significance (p) and sample size (n) for examples of significant relationships found between the percentage of sand at depth and changes in (a) beach width at MWL and (b) area within MLWS-MHWS for Transect A, and (c) change in area above MLWS for Transect C.

In comparison, very strong negative correlations were found for Transect C, between proportion of sand at depth and changes per day in area above MLWS (Figure 22c), above MWL (r=-0.85, p=0.008, n=8) and above MHWS (r=-0.90, p=0.002, n=8). A significant negative correlation was also found between change per day in area above MHWS and the proportion of sand at surface (r=-0.81, p=0.014, n=8). A similar relationship was found at Transect E, between the proportion of sand at surface and change per day in area above MWL (r=-0.71, p=0.049, n=8).

The contrasting relationships observed for Transect A and Transects C and E suggest that the critical threshold of 35% sand leading to an increase in beach erosion is not evident or, at least, is not widely applicable. Coastal settings and variations in sediment transport influence beach response in ways that may supersede the effects of reduced hydraulic conductivity. The morphological differences between the transects, particularly the settings above MHWS, influence the distribution of sand and gravel across the profile. This, combined with the effects of longshore sediment transport, may be the reasons for which statistical relationships are significant only for areas below MHWS at Transect A and above MHWS at Transect C.

Above MHWS, gravel ridges dominate in Transect A, and the variation in the proportion of sand tends to be small (Figure 23a,b) and controlled by the presence and elevation of gravel ridges. Well-formed gravel ridges migrating landward are likely to reduce the proportion of sand above MWHS and increase it below MHWS, with the movement of gravel resulting in erosion (Figure 23a). When ridges lose form and elevation, waves and gravity tend to spread the gravel along the profile reducing the relative proportion of sand at surface (Figure 23b). Accretion in Transect A associated with an increase in the proportion of sand can only occur below MHWS and due to supply from longshore sediment transport.

In the period of analysis (Aug-2016 to Mar-2018), southerly waves were dominant (Table 1). When southerly waves dominate, beach accretion is observed in the area of the ness and the adjacent nearshore, while erosion is observed at Transect C (Figure 14). When erosion at Transect C results in cliff retreat (Figure 23c,d), a considerable volume of sand is released, often increasing the proportion of sand above MHWS (Figure 23d). Modelling simulations show that, under both northerly and southerly wave conditions, sediment is transported northwards from the area of Transect C to the ness, where it is deposited due to sediment convergence (Figure 18). Therefore, the material eroded from Transect C, which is dominantly sand, tends to be deposited at the ness below MHWS (an increase in sand resulting in accretion). When northerly waves dominate, erosion is enhanced at Transect C due to a divergence of sediment (Figure 18a), which is not observed when southerly waves dominate (Figure 18b). The changes shown in Figure 23 illustrate these differences. Between 3-Aug-2016 and 6-Dec-2016 northerly waves dominated (47% of the time, southerly waves 36%), resulting in enhanced erosion at Transect C (Figure 23c). From 6-Dec-2016 to 19-Jan-2017, southerly waves dominated (55% of the time, northerly waves 29%) resulting in loss of area above MHWS and accretion below MHWS (Figure 23d).

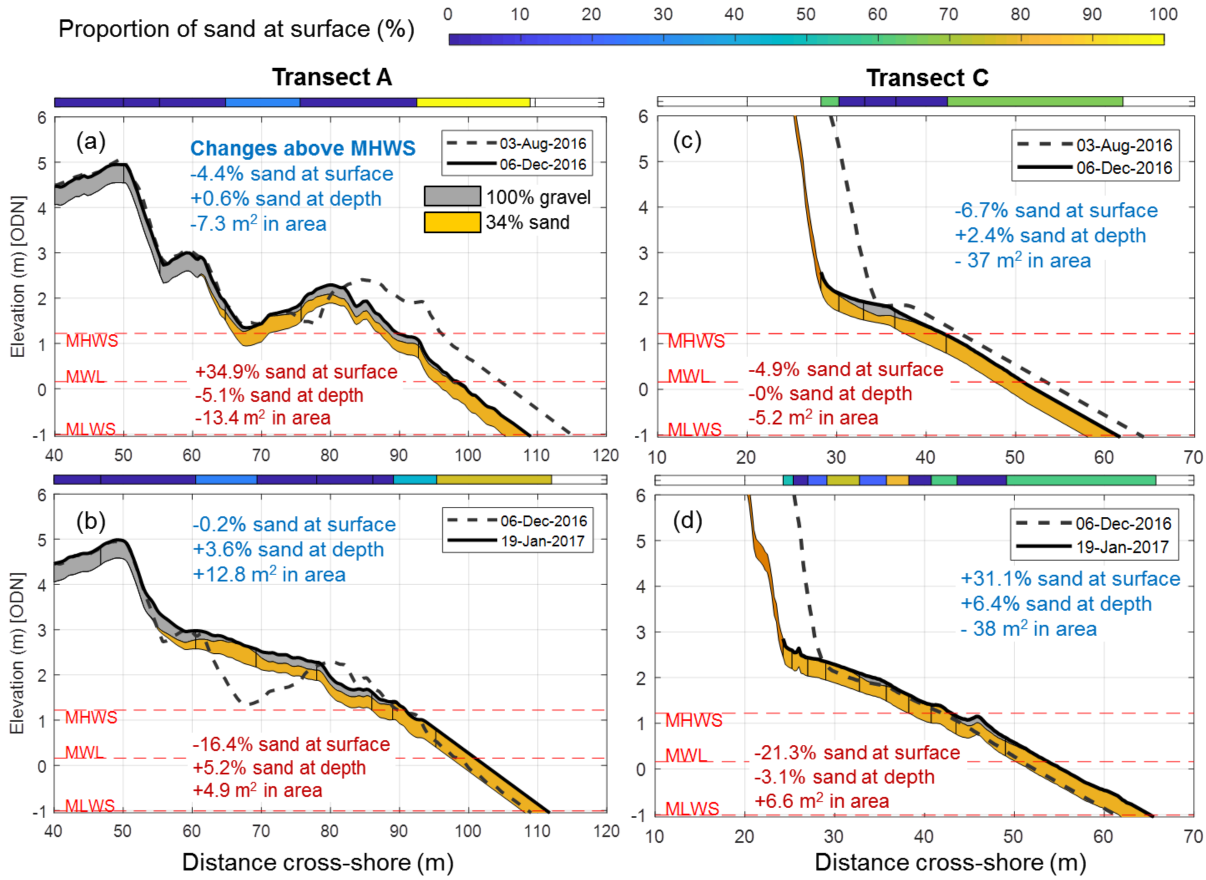

Figure 23. Examples of variation in beach profiles and the proportion of sand and gravel along Transects A on 6-Dec-2016 (a) and 19-Jan-2017 (b) and Transect C on the same dates (c and d, respectively). Changes in cross-sectional area and in the proportion of sand above and below MHWS are shown (in blue and red, respectively) in relation to a previous survey (dashed line).

8. SUMMARY OF KEY FINDINGS

X-band radar data provided valuable information on the nearshore bathymetry at temporal and spatial resolutions that helped our understanding of linkages between beach and nearshore changes. In particular, the cyclical accretion and erosion phases of the oblique bar off the ness, and the role of this feature in moderating wave climate and alongshore sediment transport has provided a new understanding of the local sediment budget. The radar data has also highlighted that the most dynamic nearshore areas are related to the formation and evolution of this oblique bar. Net changes in seabed sediment volume can be large (29,000 m^3) even over periods of only few weeks (such as between 21-Jan-2017 and 13-Feb-2017). Over longer periods, net nearshore changes across the area can reach 74,000 m^3 (observed between 11-Oct-2015 and 6-Feb-2016).

Numerical modelling has shown that under most wave and nearshore conditions, there is a persistent convergence of sediment at the ness, which contributes to its stability. It means that, in a typical year, the ness receives around 3,000 m^3 of gravel transported northwards from Thorpeness and 1,000 m^3 transported southwards from areas north of ness. On the other hand, when northerly waves dominate over prolonged periods, a divergence of sediment can enhance erosion north of Thorpeness. Under such conditions, the direction of longshore transport reverses along Thorpeness and moves sediment southwards. A sediment deficit may occur south of Thorpeness as the volume of sediment leaving that coastal stretch is greater than the volume of sediment arriving.

Analyses of 10 years of beach profile data indicate that the ness is the only area showing an overall accretion over the period. Other areas have shown a reduction from 20% to 60% in profile cross-sectional area. Periods of erosion and accretion were observed in all beach profiles, but at different timings. Periods dominated by southerly waves reduce stability along the Thorpeness beach frontage and favour accretion at the ness (more or less matching the changes observed in the nearshore). An increase in the proportion of northerly waves tends to cause erosion at the ness and north of Thorpeness and accretion in other areas. Beach erosion intensifies in all areas when northerly waves dominate and the oblique bar off the ness is in an eroded state.

Based on the results of this study, the following aspects are relevant to inform local coastal management decisions:

1. Within the study area, the ness seems the most favourable source of gravel for small-scale beach recharge operations benefitting the Thorpeness frontage. Particularly, if sediment extraction is limited to the dynamic part of the profile (below MHWS) and after periods of accretion. Material used to recharge the beach at Thorpeness is likely to return to the ness naturally through longshore transport. Therefore, it is important to carefully consider the volume and timing of the operations to ensure that they will provide coastal protection at Thorpeness without causing detrimental impacts elsewhere.
2. The area south of the ness from where gravel has been extracted in the past has experienced considerable erosion since 2014. Gravel extraction from this area should be avoided at least until the profile area is returned to pre-2014 conditions. Numerical modelling studies may be useful to identify thresholds for beach stability in this area and the associated linkages to changes elsewhere.
3. The gabions and the geobags installed to protect the North End Avenue frontage have offered some protection to the beachfront properties. However, they have reduced the beach width and the level of natural dissipation of wave energy, increasing the exposure to the defences and the beachfront properties. Further, the geobags have enhanced erosion to the north, by causing a 'terminal groyne' effect. Replacing the temporary geobags with a more permanent structure, such as a rock revetment, is very likely to enhance erosion to the north and result in further reduction in the beach width in front of the structure. Therefore, exposure to waves and risk of erosion are likely to increase in the longer-term.
4. Our results suggest that the most sustainable and less detrimental option to reduce the impact of erosion at Thorpeness in the short-term is small-scale beach recharge using the ness as a source of material as indicated above. However, if northerly waves become more dominant in the next years, this option may no longer be feasible due to changes in the local sediment budget. Further, as conditions may become more severe due to impacts of climate change, the protection of existing beachfront properties may require an increased frequency of operations and sediment volume. Therefore, for the longer-term economic and environmental sustainability of this area, management decisions need to consider measures that allow the coast to behave more naturally and prevent further

occupation and values at risk. Options may include a combination of setback lines, restrictions on property improvements that may enhance erosion or increase assets at risk, and managed realignment.

REFERENCES

Adams, J., 1979. Gravel Size Analysis from Photographs. *Journal of the Hydraulics Division*, 105 (10), 1247–1255.

Atkinson, J., 2019. Understanding the Dynamics of a Mixed Sand and Gravel Coastline: A Multi-Method Approach. PhD Thesis (submitted), Bournemouth University.

Atkinson, J., Esteves, L. S., Williams, J. W., McCann, D. L., and Bell, P. S., 2018. The Application of X-Band Radar for Characterization of Nearshore Dynamics on a Mixed Sand and Gravel Beach. *Journal of Coastal Research*, 85, 281–285.

Atkinson, J. and Esteves, L., 2018. Alongshore Variability in the Response of a Mixed Sand and Gravel Beach to Bimodal Wave Direction. *Geosciences*, 8 (12), 488.

Bunte, K. and Abt, S.R., 2001. Sampling Surface and Subsurface Particle-Size Distributions in Wadable Gravel- and Cobble-Bed Streams for Analyses in Sediment Transport, Hydraulics, and Streambed Monitoring. General Technical Report RMRS-GTR-74, Forest Service, U.S. Department of Agriculture, Fort Collins: USA, 428 p.

Burningham, H. and French, J., 2016. Shoreline-Shoreface Dynamics on the Suffolk Coast. Crown Estate.

Burningham, H. and French, J., 2017. Understanding coastal change using shoreline trend analysis supported by cluster-based segmentation. *Geomorphology*, 282, 131–149.

Carr, A. P., 1981. Evidence for the sediment circulation along the coast of East Anglia. *Marine Geology*, 40 (3), M9–M22.

Dornbusch, U., Williams, R., and Moses, C., 2005. Beach Materials Properties; BAR Phase 1, Science Report, (February 2003), 1–25.

Dunkerley, D. L., 1994. Discussion: Bulk sampling of coarse clastic sediments for particle-size analysis. *Earth Surface Processes and Landforms*, 19 (3), 255–261.

Gale, S. and Hoare, P., 1992. Bulk sampling of coarse clastic sediments for particle-size analysis. *Earth Surface Processes and Landforms*, 17 (7), 729–733.

Hey, R. D. and Thorne, C. R., 1983. Accuracy of surface samples from gravel bed material. *Journal of Hydraulic Engineering*, 109 (6), 842–851.

Horn, D. P. and Walton, S. M., 2007. Spatial and temporal variations of sediment size on a mixed sand and gravel beach. *Sedimentary Geology*, 202 (3), 509–528.

Mason, T. and Coates, T. T., 2001. Sediment Transport Processes on Mixed Beaches: A Review for Shoreline Management. *Journal of Coastal Research*, 17 (3), 645–657.

McCave, I. N., 1978. Grain-size trends and transport along beaches: Example from eastern England. *Marine Geology*, 28 (1), M43–M51.

Mott MacDonald, 2014. Thorpeness Coastal Erosion Appraisal. Mott MacDonald 347287/MMN/PCO/001/B.

Mott MacDonald, 2016. Thorpeness Coastal Protection - Options Appraisal Study. Mott MacDonald 33/PCO/1/1/3.

Van Rijn, L. C., 2014. A simple general expression for longshore transport of sand, gravel and shingle. *Coastal Engineering*, 90, 23–39.

She, K., Horn, D. P. D. P., and Canning, P., 2006. Porosity and Hydraulic Conductivity of Mixed Sand-Gravel Sediment. *Flood and Coastal Risk Management*, Conference Proceedings, 16p.

Yuzyk, T. R. and Winkler, T., 1991. *Procedures for bed-material sampling*. Lesson Package 28. Environment Canada, Water Resources Branch, Sediment Survey Section, Ottawa.

APPENDIX A: DIGITAL TERRAIN MODELS AND CHANGES IN BEACH VOLUME

Topography data obtained from laser scanner surveys were used to assess changes in beach elevation along the Thorpeness beachfrontage. Beach elevation data measured on six dates between 6-Dec-2016 and 24-Jan-2018 are represented as Digital Terreain Models (DTMs) in Figures 24 to 27 (panels a and b). Panels c show differences in beach elevation between surveys and changes in beach volume above MHWS estimated for the northern and southern sectors of the house frontage.

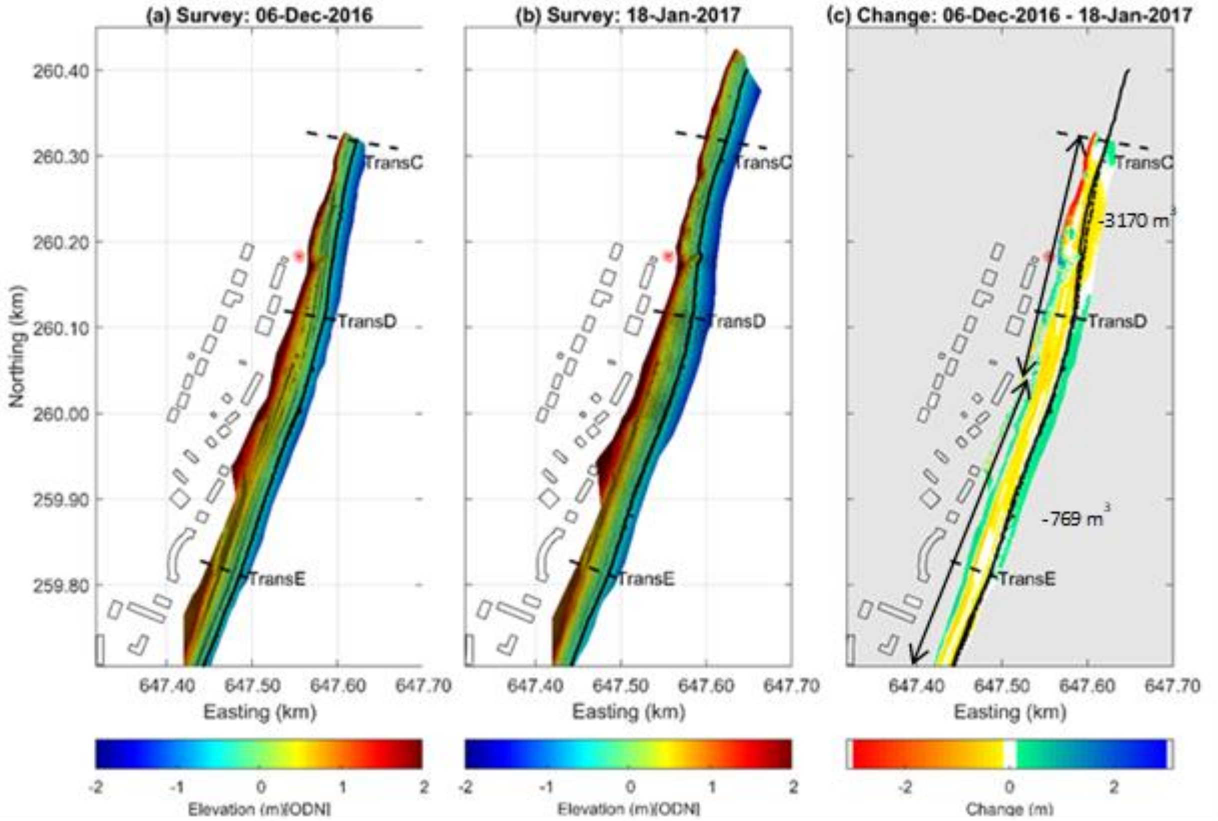

Figure 24. Beach elevation measured on (a) 06-Dec-2016 and (b) 18-Jan-2017. (c) Changes in elevation between these dates, with values indicating volume change above MHWS within the northern and southern sectors (marked by the arrows). The position of the MHWS is shown as a black line, Transects C, D and E as dashed lines and the radar as a red star.

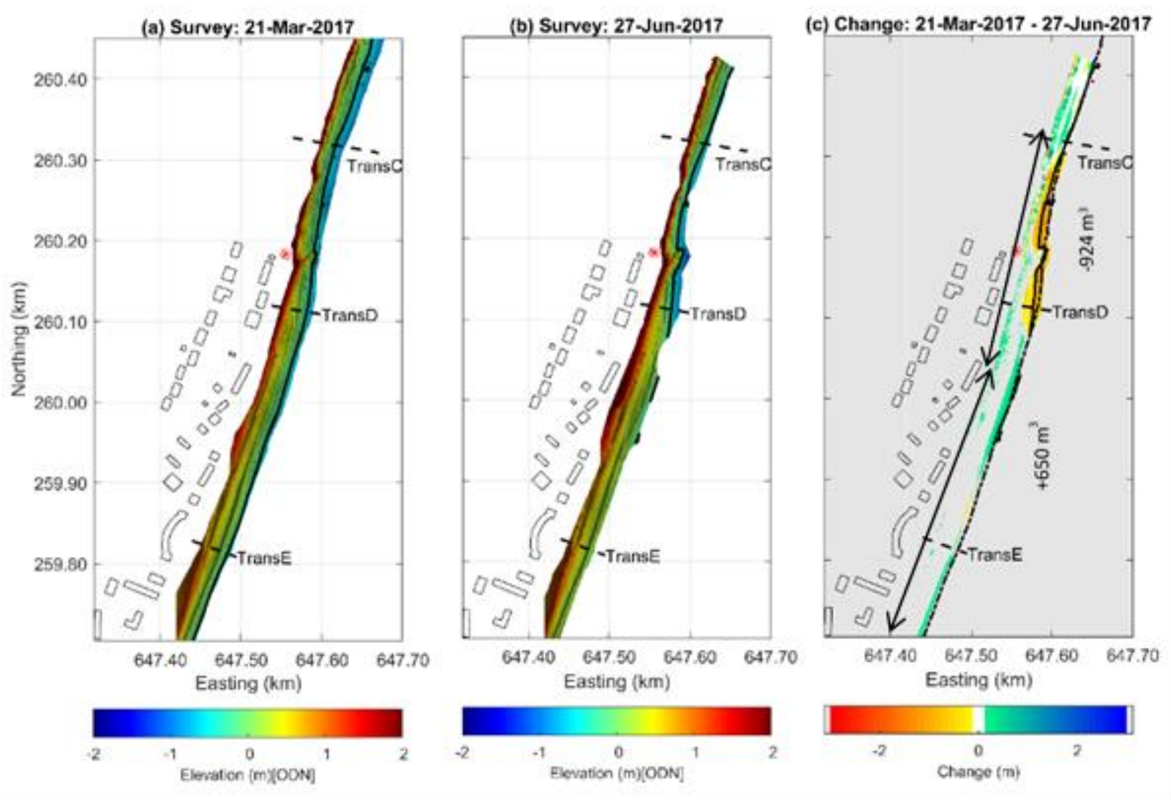

Figure 25. Beach elevation measured on (a) 21-Mar-2017 and (b) 27-Jun-2017. (c) Changes in elevation between these dates, with values indicating volume change above MHWS within the northern and southern sectors (marked by the arrows). The position of the MHWS is shown as a black line, Transects C, D and E as dashed lines and the radar as a red star.

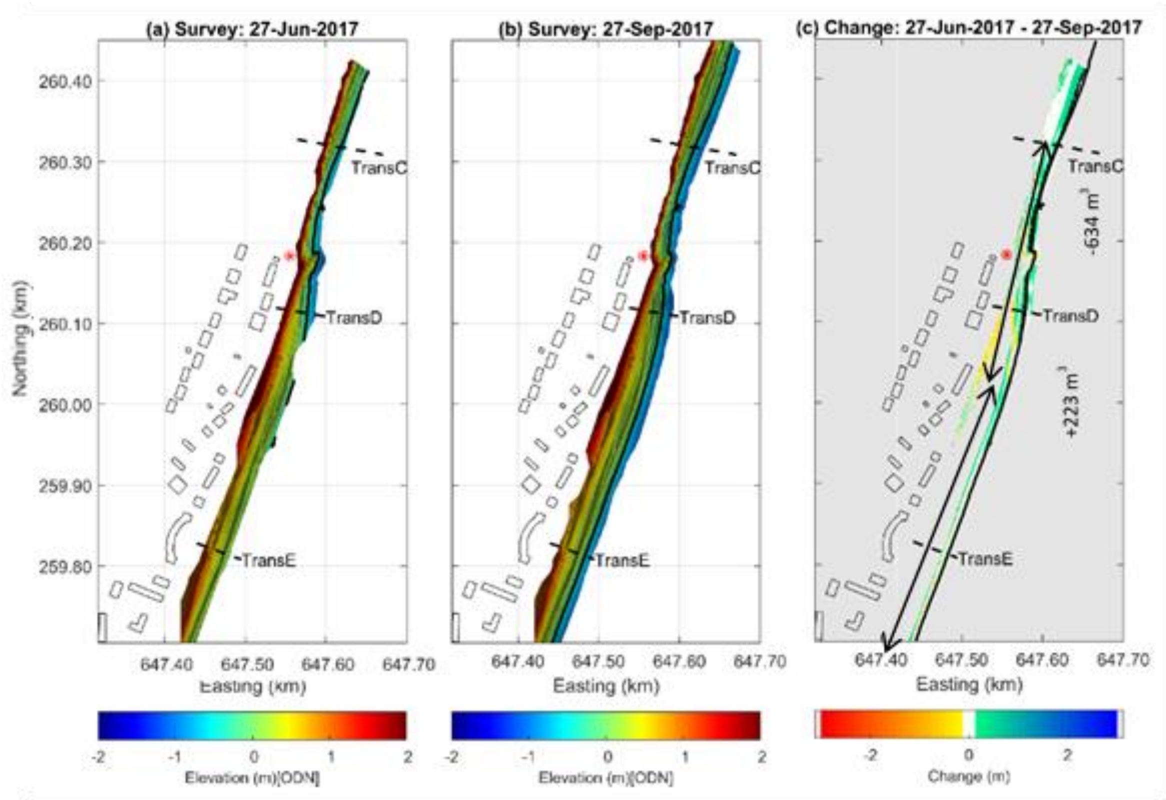

Figure 26. Beach elevation measured on (a) 27-Jun-2017 and (b) 27-Sep-2017. (c) Changes in elevation between these dates, with values indicating volume change above MHWS within the northern and southern sectors (marked by the arrows). The position of the MHWS is shown as a black line, Transects C, D and E as dashed lines and the radar as a red star.

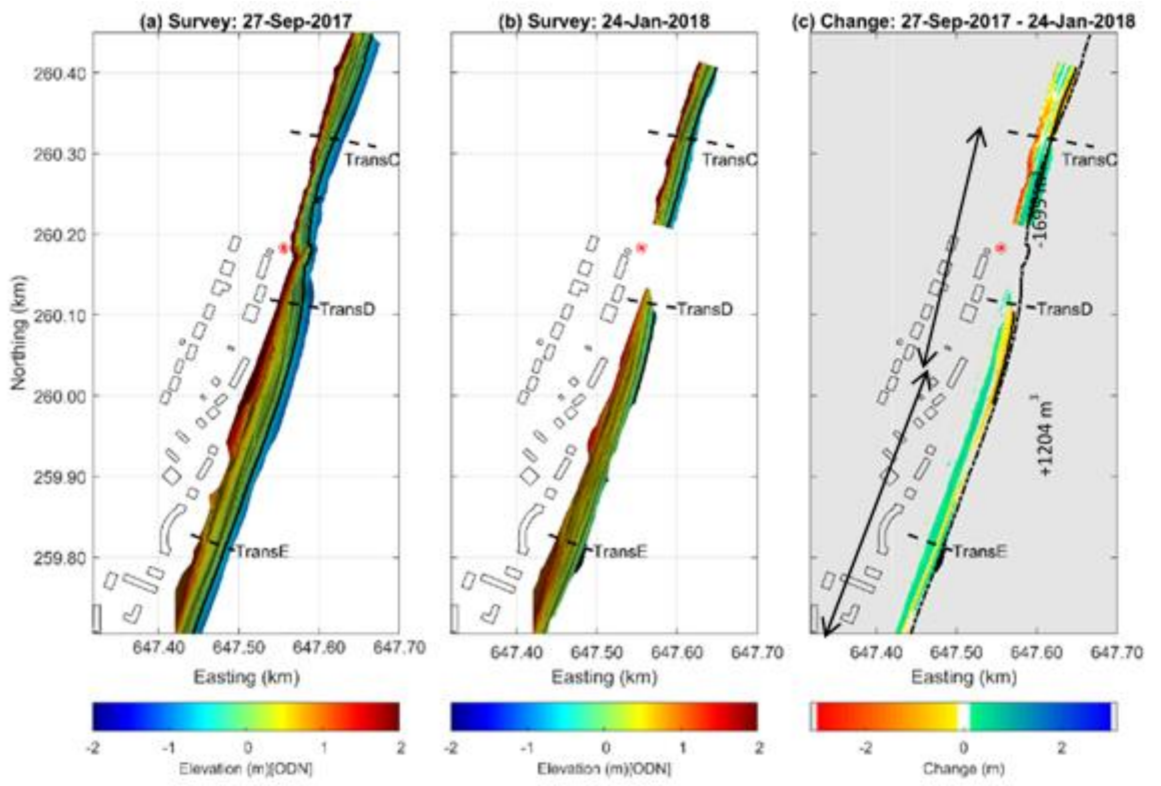

Figure 27. Beach elevation measured on (a) 27-Sep-2017 and (b) 24-Jan-2018. (c) Changes in elevation between these dates, with values indicating volume change above MHWS within the northern and southern sectors (marked by the arrows). The position of the MHWS is shown as a black line, Transects C, D and E as dashed lines and the radar as a red star.

APPENDIX B: ACCESS TO DATA

This Excel file shows the wave parameters and beach change data along Transects A to E analysed in this study. Dataset 1 covers a 10-year period focusing on surveys undertaken twice a year by the Environment Agency. Dataset 2 covers data collected at shorter-periods over two years as part of the PhD research. Beach changes are estimated as changes in beach width and profile cross-sectional area within beach compartments defined by MLWS, MWL and MHWL.

Appendix B - ProfileChange Table

APPENDIX C: CALIBRATION OF THE RADAR-DERIVED BATHYMETRY

A comparison with bathymetry obtained on the same dates by multibeam surveys allowed assessing that the accuracy of the bathymetry derived from radar data. Results indicated that the radar-derived bathymetry tends to overestimate depths in shallow waters and underestimate depths in deeper waters (Figure 28a). A linear calibration was applied resulting in 96% of the radar-derived bathymetry showing accuracy within ±0.5 m of the multibeam data and 100% within ±1 m (Figure 28b).

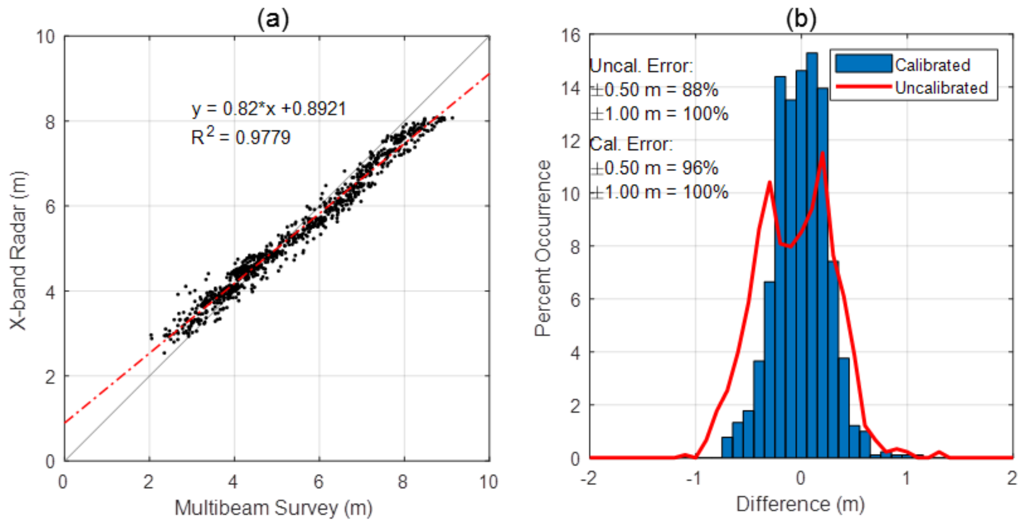

Figure 28. (a) Scatter plot of the depths derived from radar data and multibeam surveys showing linear regression line in red. (b) Histogram showing differences between multibeam bathymetry and radar derived-depths after calibration (blue) compared with the uncalibrated depth (red).